

Article

Estimation of the Hurst Parameter in Spot Volatility

Yicun Li ¹  and Yuanyang Teng ^{2,*}

¹ Business School, Zhejiang University City College, Hangzhou Yiyuan Technology Co., Ltd., Hangzhou 310015, China; 11820048@zju.edu.cn

² School of Management, Zhejiang University, Hangzhou Yiyuan Technology Co., Ltd., Hangzhou 310027, China

* Correspondence: 11620043@zju.edu.cn; Tel.: +86-183-5819-2972

Abstract: This paper contributes in three stages in a logic of the cognitive process: we firstly propose a new estimation of Hurst exponent by changing frequency method which is purely mathematical. Then we want to check if the new Hurst is efficient, so we prove the advantages of this new Hurst in asymptotic variance in the perspective compared with other two Hurst estimator. However, a purely mathematical game is not enough, a good estimation should be proven by reality, so we apply the new Hurst estimator into truncated and non-truncated spot volatility which fills the gap of previous literatures using 5-min price data (Source: Wind Financial Terminal) of 10 Chinese A-share industry indices from 1 January 2005 until 31 December 2020.

Keywords: spot volatility; change of frequency; roughness of volatility; hurst exponent; Chinese A-share market

MSC: 60F17; 91B70



Citation: Li, Y.; Teng, Y. Estimation of the Hurst Parameter in Spot Volatility. *Mathematics* **2022**, *10*, 1619. <https://doi.org/10.3390/math10101619>

Academic Editors: Camelia Petrescu and Valeriu David

Received: 7 April 2022

Accepted: 7 May 2022

Published: 10 May 2022

Publisher's Note: MDPI stays neutral with regard to jurisdictional claims in published maps and institutional affiliations.



Copyright: © 2022 by the authors. Licensee MDPI, Basel, Switzerland. This article is an open access article distributed under the terms and conditions of the Creative Commons Attribution (CC BY) license (<https://creativecommons.org/licenses/by/4.0/>).

1. Introduction

Since the seminal work of Black and Scholes [1], the price dynamics described by the following equation have been well-known to researchers in the fields.

$$d\log S_t = \mu_t dt + \sigma_t dW_t,$$

where μ_t is a drift process, σ_t depicts the volatility process and W_t is standard Brownian motion. Since the constant volatility assumption of the model in Black and Scholes [1] contradicts empirical observation (see, for example, Fouque et al. [2]), more and more innovative models are proposed (see Hull and White [3]; Scott [4]; Stein and Stein [5]).

Despite these improvements in the above-mentioned stochastic volatility models, empirical studies have underlined the long-memory feature of the volatility of financial assets. To address this issue, a natural idea is to replace Brownian motion in the volatility process by fractional Brownian motion (fBm), which can describe the long memory property with the Hurst parameter $0.5 < H < 1$. Hence, Comte and Renault [6] proposed a fractional version of the Hull-White stochastic volatility model with the Hurst parameter $H > 0.5$ in fBm to model log-volatility and consider the option pricing problem in a long memory volatility environment. Other related research has been conducted by Comte et al. [7], Chronopoulou and Viens [8], Chronopoulou and Viens [9], Xiao and Yu [10].

Recent empirical studies have documented the roughness of historical volatility data and the implied roughness of option price data (see, e.g., Bennedsen et al. [11]; Bayer et al. [12]; Gatheral et al. [13]; Livieri et al. [14]; El Euch and Rosenbaum [15]). Early research conducted by Alòs et al. [16] investigated the short-time behavior of implied volatility by jump-diffusion models. Compared with Alòs et al. [16], Fukasawa and Takabatake [17] discussed self-similar stationary Gaussian noises such as fractional Gaussian noises, which indicate the volatility series. They extended the Whittle estimation method to

obtain asymptotically efficient estimators. Moreover, many studies have evaluated realized volatility forecasting performance of several models (see, e.g., Li et al. [18]; Wang et al. [19]; Wang et al. [20]) More precisely, Gatheral et al. [13] calibrated a model to the SP500 and NASDAQ indices, showing that the Hurst parameter of volatility should be close to 0.11. Other important indices, including the FTSE2, N2252, RUT2, DJI2, FCHI2, KS11, SSML, IBEX2, NSEI, MXX, BVSP, GSPTSE, STOXX50E, FTSTI, FTSEMIB have also been studied. This indicates extremely rough directions for the volatility process, being much more irregular than those of standard stochastic volatility models driven by Brownian motion. Further empirical studies have confirmed the roughness of the log-volatility of thousands of stocks on the US equity market (Bennedsen et al. [11]). Livieri et al. [14] found that at-the-money short term volatility from SP500 options is also rough. Using high-frequency data for major volatility indices and the q th-order structure function (SF) method proposed by Gatheral et al. [13], Da Fonseca and Zhang [21] computed the volatility of major indices in the USA and showed the roughness of the volatility of volatility. Cao et al. [22] showed that even the elasticity of variance for the SP500 is rough. Takaishi [23] verified the roughness of Bitcoin volatility using MF-DFA based on Bitcoin tick data. Bennedsen et al. [11] verified the volatility roughness of many stocks. It has been shown recently that both the realized volatility and the option-implied volatility are rough. Recently, Fukasawa et al. [24] used a quasi-likelihood estimator to estimate the Hurst parameter of the S&P 500, FTSE 100, Nikkei 225, DAX, and Russell 3000 indices and found that the volatility is rough. Brandi and Di Matteo [25] computed the Hurst exponent on realized variance from the Oxford volatility library and found that the volatility is indeed rough with a Hurst exponent between 0.08 and 0.15. Alòs and León [26] provided a comprehensive discussion of rough volatility. With research progressing, spot volatility catches the eyes of researchers. Efficient estimation of spot volatility can be achieved by using Riemann-like integration. Applications of spot volatility are of great importance. For example, spot volatility can be used to detect the micro-structure of the of financial assets. It was also useful to explain jumps and co-jumps of volatility series as shown by Jacod and Todorov [27]. Moreover, spot volatility can be calibrated to implied volatility and play a key role in the option pricing. There are many publications about spot volatility in which it has been extensively studied (see, e.g., Fan and Wang [28]; Reno [29] and references therein).

This paper focuses on the roughness of spot volatility and proposes some interesting contributions:

- We propose a new Hurst exponent by changing the frequency method, prove consistency, and derive the asymptotic volatility of our estimator. Then we do simulations by the Monte Carlo method and compare our new Hurst estimator with existing Hurst exponents, showing its advantages.
- We introduce a non-parametric estimator for spot volatility based on the rough volatility environment proposed by Bayer et al. [12], and Gatheral et al. [13]. While Fan and Wang [28] proposed the same non-parametric estimator for spot volatility based on fractional stochastic volatility models with $H \in (1/2, 1)$, we extend this estimator for all $H \in (0, 1)$. The proof method established in this paper can be also applied to a general fractional stochastic volatility model with a bounded drift term.
- We employ the MF-DFA method proposed by Kantelhardt et al. [30] and q th-order SF method used by Gatheral et al. [13] to analyze the roughness of 10 industrial indices' spot volatility in the Chinese financial market. Then we compared two Hurst exponents of the least square method proposed by Berzin et al. [31] with our new Hurst exponents using empirical data. Gatheral et al. [13] proved the SF method in American markets, and their numeric results are similar to ours in Chinese markets. There is much evidence showing the roughness of volatility in different sectors and markets (see Guennoun et al. [32], Funahashi and Kijima [33], Neuenkirch and Shalaiko [34]). We confirmed that the Hurst exponent we propose is universal in other markets and sectors. Our results suggest that spot volatility is also rough, and has confirmed the

roughness of realized volatility (Bennedsen et al. [10]; Gatheral et al. [13]) and implied volatility (Livieri et al. [14]).

The rest of this paper is organized as follows. Section 2 introduces the non-parametric estimator for spot volatility from the rough stochastic volatility model proposed by Bayer et al. [12], and Gatheral et al. [13] and provides the asymptotic theory for the proposed non-parametric estimator. Section 3 presents the new estimator and investigates its asymptotic properties. Four popular methods for estimating the generalized Hurst exponent are also introduced in the later part of this Section. Section 4 presents some empirical studies. Section 5 discusses the contribution of this study with other research in the literature. Section 6 outlines the conclusion of our analysis. Components of proofs are collected in Appendix A.

2. The Spot Volatility Model

Modeling rough volatility is becoming increasingly popular and has important applications in finance. This is because rough volatility models must fit the volatility skew, which is defined as the derivative of the implied volatility surface under the Black-Scholes-Merton model with respect to log-strike price evaluated at-the-money. Moreover, rough volatility models must satisfy the mono-fractal scaling property of the historical volatility data, which means that for a given lag Δ , each q -th sample moment of the differences of log-volatility exhibits a power-scaling relationship with respect to this lag, i.e., $|\log \sigma_{t+\Delta_n} - \log \sigma_t|^q \propto \Delta^{qH}$ with $q > 0$ and $\Delta > 0$. Consequently, rough volatility models have important applications in finance, and the literature on estimating spot volatility is large. From the celebrated rough volatility model by Bayer et al. [12], Gatheral et al. [13] and Xiao and Yu [10], we assume that the asset price S_t follows the following dynamic:

$$\begin{cases} \frac{dS_t}{S_t} = \mu_t dt + \sigma_t dW_t \\ \sigma_t = \exp\{X_t\}, t \in [0, T] \\ dX_t = \alpha(m - X_t)dt + \nu dB_t^H \end{cases} \quad (1)$$

where S_t and σ_t are the price and volatility processes, respectively. Moreover, μ_t is a suitable drift term and satisfies $\sup\{|\mu_t - \mu_s|, |t - s| \leq a\} = O_P(a^{1/2} |\log a|_{1/2})$, σ is the diffusion term, i.e., the spot volatility of the stock, $\alpha > 0$ is the speed of mean-reversion, m is the long term level of the variance, ν is the volatility of volatility, W_t is a Wiener process, i.e., a Brownian motion, and B_t^H is a fBm with Hurst parameter $H \in (0, 1)$. Following the idea of Bayer et al. [12] and Gatheral et al. [13], we assume that B_t^H is independent of W_t .

The model of (1) can describe both the mean reverting property and the roughness of the volatility. The self-similarity parameter, also called the Hurst parameter in the fBm, is a crucial criterion to test the roughness of the volatility. Consequently, estimating the Hurst parameter in the volatility has been the subject of active research and a challenging theoretical problem. In the literature, there exist many approaches for estimating the Hurst parameter, such as rescaled range, aggregated variance, aggregated absolute value, variance of residuals, log-periodogram regression, Whittle estimation, local Whittle estimation, novel time-varying generalized Hurst exponent methodology (see, for example, Kermarrec [35], Keshari Jena et al. [36], and Xiao et al. [37]) and so on. In this paper, we use MF-DFA proposed by Kantelhardt et al. [30] and the q -th order SF introduced by Gatheral et al. [13]. In what follows, we first introduce a non-parametric estimator for spot volatility in (1) then we introduce two methods for estimating the Hurst parameter.

The recent availability of high frequency data in finance has permitted more efficient ways of computing spot volatility. However, the estimation of the spot volatility from asset price observations is challenging because observed high frequency data are generally affected by noise-microstructure effects. Hence, following Fan and Wang [28], this subsection is devoted to the nonparametric estimation method for spot volatility in a rough volatility environment, which yields suboptimal convergence rates.

For any positive integer n , let $\Delta = T/n$ and $K(x)$ be a kernel with $\int_{-1}^1 K(x)dx = 1$. Moreover, suppose that we observe S_{t_i} at n discrete time points with $t_i = i\Delta = iT/n$,

$i = 1, 2, \dots, n$. Then, following the idea of Fan and Wang [28], we define the kernel type estimator for the spot volatility as:

$$\hat{\sigma}_t := \sqrt{\frac{1}{b} \sum_{t_i=t-b}^{t+b} K\left(\frac{t_i-t}{b}\right) (S_{t_i} - S_{t_{i-1}})^2} \tag{2}$$

where b is a bandwidth.

The estimator (2) will be used for the continuous case as it is not jump robust and not noise robust. From Christensen et al. [38], we can see that the impact of jumps is negligible in the data studied here. Moreover, 5-min sampling data is commonly used and not affected by market micro-structure noise. Fan and Wang [28] impose the following assumptions for μ_t , σ_t and $K(x)$ provided by the following result.

When the price process is assumed to be present with jumps, the truncated estimator $\bar{\sigma}_t$ for the spot volatility can be calculated as:

$$\bar{\sigma}_t(k_n, \nu_n) = \sqrt{\frac{1}{k_n \Delta_n} \sum_{i=0}^{k_n-1} \left(Y_{(m+1+i)\Delta_n} - Y_{(m+i)\Delta_n} \right)^2 \mathbf{1}_{\{|Y_{(m+1+i)\Delta_n} - Y_{(m+i)\Delta_n}| \leq \nu_n\}}} \tag{3}$$

Hypothesis 1. Suppose the following conditions are satisfied:

A1 The diffusion term σ_t in (1) satisfies:

$$\sup\{|\sigma_s - \sigma_t|, |s - t| \leq a\} = O_{\mathbb{P}}(a^{1/2} |\log a|_{1/2}) \text{ and } \sup_{0 \leq t \leq T} |\sigma_t^2| = O_{\mathbb{P}}(1).$$

A2 For $i = 1, 2, \dots, n$, $\sup\{|\int_{t_{i-1}}^{t_i} (\sigma(s) - \sigma(t_{i-1})) dW_s|^2\} = O_{\mathbb{P}}(n^{-2+\eta})$, where η is an arbitrarily small number.

A3 The drift term μ_t in (1) satisfies:

$$\sup\{|\mu_t - \mu_s|, |t - s| \leq a\} = O_{\mathbb{P}}(a^{1/2} |\log a|_{1/2})$$

A4 Bandwidth b and kernel K satisfy $b \sim n^{-1/2} / \log(n)$, $K(\cdot)$ is twice differentiable with support $[1, 1]$ and $\int_{-1}^1 K(x) dx = 1$.

From Cheridito et al. [39], and for $\alpha > 0$, we can see that $X_t = \log(\sigma_t)$ defined by (1) is a stationary and ergodic if one chooses a suitable initial condition $X_0 = \mu + \sigma \int_{-\infty}^0 e^{ks} dB_s^H$. Moreover, we have the following important result.

Lemma 1. For $\alpha > 0$, the random variable $X_t = \log(\sigma_t)$ has normal distribution with mean $(1 - e^{-\alpha t})m + X_0 e^{-\alpha t}$ and

$$\text{Var} X_t = H\nu^2 \int_0^t z^{2H-1} (e^{-\alpha z} + e^{-\alpha(2t-z)}) dz \tag{4}$$

To verify the assumptions in Hypothesis 1, we state the following technical lemma.

Lemma 2. For all $H \in (0, 1)$ and any $p \geq 1$, there exist positive constants C , such that

$$\mathbb{E}|X_t|^p \leq C \tag{5}$$

$$\mathbb{E}|X_t - X_s|^p \leq C|t - s|^{pH} \tag{6}$$

for all $t, s \geq 0$.

We show below that Assumptions A1 and A2 of σ_t in Hypothesis 1 are satisfied for the volatility process in (1) as well as its super-positions.

Lemma 3. *Suppose that the volatility process is described by X_t in (1). Then conditions A1 and A2 in Hypothesis 1 are satisfied.*

Now, using the definition of μ_t and $K(x) = e^x 1_{(x \leq 0)}$, we can see that A3 and A4 in Hypothesis 1 are satisfied. Under assumption 1, Fan and Wang [28] provided the asymptotic theory for $\hat{\sigma}_t$, which is proposed by the following result.

Proposition 1. *Under the Hypothesis 1, we have:*

$$\sqrt{nb}(\hat{\sigma}_t^2 - \sigma_t^2) \xrightarrow{d} N\left(0, \sigma_t^4 \int_{-1}^1 K^2(x) dx\right) \tag{7}$$

where \xrightarrow{d} denotes convergence in distribution and $K(x)$ is defined in A4 of Hypothesis 1.

Moreover, let $M_n = \sup_{0 \leq t \leq T} \sqrt{nb} \|\hat{\sigma}_t^2 - \sigma_t^2\|$ and $\lambda(k) = \int_{-1}^1 K^2(x) dx$ If σ_t is a stationary process, then we have

$$(2 \log n)^{1/2} \left(\frac{M_n}{\sqrt{\int_{-1}^1 K^2(x) dx}} - d_n \right) \xrightarrow{d} \exp(-2e^{-x}) \tag{8}$$

where

$$d_n = \begin{cases} (2 \log n)^{1/2} + \frac{\log \lambda_1(K) - 0.5 \log \pi - 0.5 \log(\log n)}{(2 \log n)^{1/2}}, & \text{if } \frac{K^2(-1) + K^2(1)}{2\lambda(K)} > 0 \\ (2 \log n)^{1/2} + \frac{\log\left(\frac{1}{2\lambda(K)} \int [K'(x)]^2 dx\right) - \log(2\pi)}{(2 \log n)^{1/2}}, & \text{otherwise.} \end{cases} \tag{9}$$

Remark 1. *The class of kernels $K(\cdot)$ which are allowed for the asymptotic theory in Proposition 2.1 include those in the existing literature. From Fan and Wang [28], we impose differentiability and some kind of Lipschitz regularity for $K(\cdot)$. Prominent kernel functions, such as the Gaussian kernel allow for the asymptotic theory in Proposition 1.*

Remark 2. *Using Proposition 1, we can construct an asymptotic confidence band for the unknown spot volatility process.*

Remark 3. *For the asymptotic theory of spot volatility in (2), we have to eliminate the jumps on inference for spot volatility. In the case of jump activity, we can use truncated power variations and multipower variations to eliminate the jumps asymptotically. In fact, whether we allow for discontinuous price processes or not, it is quite crucial from a statistical point of view, since the existence of jumps requires a significant modification of the involved statistics to ensure jump robustness. The extension of jumps is complicated and will be reported in later work.*

Remark 4. *Micro-structure noise in high-frequency data is a commonly accepted fact. The theory presented in Fan and Wang [28] is clearly not noise-robust. The extension of their theory to noise-robust estimators is a challenging but very interesting question.*

Remark 5. *Following the idea of Bayer et al. [11] and Gatheral et al. [13], we assume that there is no leverage effect in (1). Thus, the Brownian motion and the fBm in (1) are independent. Establishing the asymptotic theory of the estimator for the spot volatility in (1) will be pursued in a future study.*

3. Estimation Methods of the Hurst Exponent

In the literature, there exist many papers that describe different methods for estimating the Hurst parameter. For example, the parameter estimation method includes the exact maximum likelihood estimation and Whittle the maximum likelihood estimation. Semi-parametric estimation approaches involve the celebrated R/S statistic method, the modified R/S statistic method, Higuchi’s method, detrended fluctuation analysis, the log-periodogram regression method and the local Whittle method. Non-parametric estimation includes the increment ratio method, the wavelet-based method and the quadratic variations approach. In this paper, we first introduce a new estimator, which is based on the change of frequency.

3.1. A New Hurst Exponent H_n

In this section we propose a new Hurst exponent estimator, which is:

$$\hat{H}_n = \frac{1}{2} - \frac{1}{2 \ln 2} \ln \left(\frac{\sum_{k=1}^{2n-1} (\Delta_{2n,k}^{(2)} X)^2}{\sum_{k=1}^{n-1} (\Delta_{n,k}^{(2)} X)^2} \right)$$

where

$$\Delta_{n,k}^{(2)} X = X(t_{k+1}^n) - 2X(t_k^n) + X(t_{k-1}^n) \text{ and } t_k^n = kT/n$$

From the equation above, we have:

$$\hat{H}_n \rightarrow H \text{ a.s.}$$

$$2 \ln 2 \sqrt{n} (\hat{H}_n - H) \xrightarrow{d} \mathcal{N}(0; \sigma_H^2), \sigma_H^2 = \frac{3}{2} \Sigma_{11} - 2 \Sigma_{12}.$$

$$\Sigma_{11} = 2 \left(1 + \frac{2}{(4-2^{2H})^2} \sum_{j=1}^{\infty} \hat{\rho}_H^2(j) \right), \Sigma_{22} = \frac{1}{2} \Sigma_{11},$$

$$\Sigma_{12} = \Sigma_{21} = \frac{1}{2^{2H} (4-2^{2H})^2} \sum_{j \in \mathbb{Z}} \tilde{\rho}_H^2(j),$$

$$\hat{\rho}_H(j) = \frac{1}{2} [-6|j|^{2H} - |j-2|^{2H} - |j+2|^{2H} + 4|j-1|^{2H} + 4|j+1|^{2H}],$$

$$\tilde{\rho}_H(j) = \frac{1}{2} [|j+1|^{2H} + 2|j+2|^{2H} - |j+3|^{2H} + |j-1|^{2H} - 4|j|^{2H} - |j-3|^{2H} + 2|j-2|^{2H}].$$

Set $B^H = \{B^H(t) : t \in [0, T]\}$, $T > 0$ as fBm.

We obtain:

$$V_{in,T}^{\hat{B}^H} = \sum_{k=1}^{in-1} (\Delta_{in,k}^{(2)} \hat{B}^H)^2, \Delta_{in,k}^{(2)} \hat{B}^H = \frac{\Delta_{in,k}^{(2)} B^H}{\sqrt{E(\Delta_{in,k}^{(2)} B^H)^2}} \quad i = 1, 2,$$

$$d_{k,j}^{\hat{B}^H, in} = E \Delta_{in,k}^{(2)} \hat{B}^H \Delta_{in,j}^{(2)} \hat{B}^H, 1 \leq j, k \leq in - 1, i = 1, 2,$$

$$c_{j,k}^{\hat{B}^H, 2n} = E \Delta_{n,j}^{(2)} \hat{B}^H \Delta_{2n,k}^{(2)} \hat{B}^H, 1 \leq j \leq n - 1, 1 \leq k \leq 2n - 1,$$

$$\Delta_{in,k}^{(2)} \hat{B}^H = \hat{B}_{\frac{k+1}{in}T}^H - 2\hat{B}_{\frac{k}{in}T}^H + \hat{B}_{\frac{k-1}{in}T}^H, 1 \leq k \leq in - 1, i = 1, 2.$$

Then we have following conclusion:

Theorem 1. Suppose $B^H = \{B^H(t) : t \in [0, T]\}$, $T > 0$ is fBm, then:

$$\mathbf{X}_n = \sqrt{n} \begin{pmatrix} n^{-1} V_{n,T}^{\hat{B}^H} - 1 \\ (2n)^{-1} V_{2n,T}^{\hat{B}^H} - 1 \end{pmatrix} \xrightarrow{d} \mathcal{N}(0; \Sigma_H), \Sigma_H = \begin{pmatrix} \Sigma_{11} & \Sigma_{12} \\ \Sigma_{12} & \Sigma_{22} \end{pmatrix}$$

where $\mathcal{N}(0; \Sigma_H)$ is a Gaussian vector:

$$\begin{aligned} \Sigma_{11} &= 2\left(1 + \frac{2}{(4-2^{2H})^2} \sum_{j=1}^{\infty} \hat{\rho}_H^2(j)\right), \Sigma_{22} = \frac{1}{2}\Sigma_{11}, \\ \Sigma_{12} = \Sigma_{21} &= \frac{1}{(4-2^{2H})^2} \sum_{j \in \mathbb{Z}} \tilde{\rho}_H^2(j), \\ \hat{\rho}_H(j) &= \frac{1}{2}[-6|j|_{2H} - |j-2|_{2H} - |j+2|_{2H} + 4|j-1|_{2H} + 4|j+1|_{2H}], \\ \tilde{\rho}_H(j) &= \frac{1}{2^{2H+1}}[|j+1|^{2H} + 2|j+2|^{2H} - |j+3|^{2H} + |j-1|^{2H} - 4|j|^{2H} \\ &\quad - |j-3|_{2H} + 2|j-2|_{2H}]. \end{aligned}$$

Proof. The proof is similar to the proof of Theorem 4 in Kubilius [40]. However, since our result is slightly different from that in Kubilius [40], we provide brief derivations here.

To determine limiting distribution of \mathbf{X}_n , we compute a limiting moment generating function $\lim M_{\mathbf{X}_n}(\lambda) = M(\lambda)$.

Consider a centered Gaussian vector $G_n = (G_n^{(i)}, 1 \leq i \leq 3n-2)$

$$\begin{aligned} G_n^{(i)} &= \Delta_{n,i}^{(2)} \hat{B}^H, 1 \leq i \leq n-1, \\ G_n^{(i)} &= \sqrt{2^{-1}} \Delta_{2n,i+1-n}^{(2)} \hat{B}^H, n \leq i \leq 3n-2 \end{aligned}$$

And a diagonal matrix:

$$D_n = \text{diag} \left(\underbrace{\lambda_1, \dots, \lambda_1}_{n-1}, \underbrace{\lambda_2, \dots, \lambda_2}_{2n-1} \right)$$

It is evident that $E G_n^{(i)} = 0$ and $E(G_n^{(i)})^2 = 1$ for all $1 \leq i \leq n-1$, $E(G_n^{(i)})^2 = 2^{-1}$ for all $n \leq i \leq 3n-2$. We denote the covariance matrix of the vector G_n by Σ_{G_n} .

Set:

$$\tilde{D}_n = (\Sigma_{G_n}^{1/2})^T D_n \Sigma_{G_n}^{1/2}$$

We give bound on eigenvalues of \tilde{D}_n . It is obvious that \tilde{D}_n is symmetric. Denote by $\|A_n\| = \sup_{\|x\|=1} \|A_n x\|$ matrix A norm. For symmetric matrix \tilde{D}_n its norm is equal to its spectral norm, i.e., $\|\tilde{D}_n\| = \rho(\tilde{D}_n) := \max_k |\lambda_k(\tilde{D}_n)|$. Since norm $\|\cdot\|$ is submultiplicative norm then:

$$\begin{aligned} \max_k |\lambda_k(\tilde{D}_n)| &= \|\tilde{D}_n\| \leq \|\Sigma_{G_n}^{1/2}\| \cdot \|D_n\| \cdot \|\Sigma_{G_n}^{1/2}\| = \|\Sigma_{G_n}^{1/2}\|^2 \cdot \|D_n\| \\ &= \rho((\Sigma_{G_n}^{1/2})^2) \cdot \rho(D_n) = \rho(\Sigma_{G_n}) \cdot \rho(D_n) = \lambda_{\max}(\Sigma_{G_n}) \cdot \max\{|l_1|, |l_2|\} \end{aligned}$$

Now consider $\lambda_{\max}(\Sigma_{G_n})$. In order to bound the maximal eigenvalue, we again make use of the fact that the latter does not exceed the maximal row sum of absolute values. Thus:

$$\lambda_{\max}(\Sigma_{G_n}) \leq \max_j \sum_{i=1}^{3n-2} |(\Sigma_{G_n})_{ij}|$$

Note that:

$$\begin{aligned} (\Sigma_{G_n})_{i,j+1-n} &= \frac{1}{\sqrt{2}} E \left[\Delta_{n,i}^{(2)} \hat{B}^H \Delta_{2n,j+1-n}^{(2)} \hat{B}^H \right] \\ &= \frac{1}{\sqrt{2}} E \left[\left(\Delta_{2n,2i+1}^{(2)} \hat{B}^H + \Delta_{2n,2i-1}^{(2)} \hat{B}^H + 2\Delta_{2n,2i}^{(2)} \hat{B}^H \right) \Delta_{2n,j+1-n}^{(2)} \hat{B}^H \right] \\ &= \frac{1}{\sqrt{2}} \left[d_{2i+1,j+1-n}^{\hat{B}^H, 2n} + d_{2i-1,j+1-n}^{\hat{B}^H, 2n} + 2d_{2i,j+1-n}^{\hat{B}^H, 2n} \right] \end{aligned}$$

For $1 \leq i \leq n - 1$ and $1 \leq j \leq 2n - 1$, from Equations above, we can obtain:

$$\begin{aligned} \lambda_{\max}(\Sigma_{\mathbf{G}_n}) &\leq \max_{1 \leq j \leq n-1} \sum_{i=1}^{n-1} |d_{i,j}^{\hat{B}^H, n}| + \frac{1}{2} \max_{1 \leq j \leq 2n-1} \sum_{i=1}^{2n-1} |d_{i,j}^{\hat{B}^H, 2n}| \\ &\quad + \frac{1}{\sqrt{2}} \max_{1 \leq j \leq n-1} \sum_{i=1}^{2n-1} \left(|d_{i,2j+1}^{\hat{B}^H, 2n}| + |d_{i,2j-1}^{\hat{B}^H, 2n}| + 2|d_{i,2j}^{\hat{B}^H, 2n}| \right) \\ &\quad + \frac{1}{\sqrt{2}} \max_{1 \leq j \leq 2n-1} \sum_{i=1}^{n-1} \left(|d_{2i+1,j}^{\hat{B}^H, 2n}| + |d_{2i-1,j}^{\hat{B}^H, 2n}| + 2|d_{2i,j}^{\hat{B}^H, 2n}| \right) \\ &\leq \max_{1 \leq j \leq n-1} \sum_{i=1}^{n-1} |d_{i,j}^{\hat{B}^H, n}| + \left(\frac{1}{2} + \frac{8}{\sqrt{2}} \right) \max_{1 \leq j \leq 2n-1} \sum_{i=1}^{2n-1} |d_{i,j}^{\hat{B}^H, 2n}| \leq 20 \end{aligned}$$

Summing up, we come to conclusion that $\max_k |\lambda_k(\tilde{D}_n)|$ is uniformly (in n, k) bounded by a finite constant depending only on λ_1, λ_2 .

Note that:

$$\lambda^T \mathbf{Y}_n := \sqrt{n}(\lambda_1, \lambda_2) \begin{pmatrix} n^{-1} (V_{n,T}^{\hat{B}^H} - EV_{n,T}^{\hat{B}^H}) \\ (2n)^{-1} (V_{2n,T}^{\hat{B}^H} - EV_{2n,T}^{\hat{B}^H}) \end{pmatrix} = \frac{1}{\sqrt{n}} (\mathbf{G}_n^T D_n \mathbf{G}_n - E \mathbf{G}_n^T D_n \mathbf{G}_n)$$

Recall that $\mathbf{G}_n \stackrel{d}{=} \sqrt{\Sigma_{\mathbf{G}_n}} \mathbf{Z}_n$ with $\mathbf{Z}_n \sim \mathcal{N}(0; I_{3n-2})$, where I_{3n-2} denotes an identity $3n - 2$ matrix. So, one can determine the following equality:

$$\mathbf{G}_n^T D_n \mathbf{G}_n \stackrel{d}{=} (\Sigma_{\mathbf{G}_n}^{1/2} \mathbf{Z}_n)^T D_n \Sigma_{\mathbf{G}_n}^{1/2} \mathbf{Z}_n = \mathbf{Z}_n^T (\Sigma_{\mathbf{G}_n}^{1/2})^T D_n \Sigma_{\mathbf{G}_n}^{1/2} \mathbf{Z}_n = \mathbf{Z}_n^T \tilde{D}_n \mathbf{Z}_n$$

Let $\tilde{D}_n = Q_n^T \Lambda(\tilde{D}_n) Q_n$ be canonical representation of \tilde{D}_n via a diagonal matrix of eigenvalues and a corresponding orthogonal matrix of eigenvectors. Since the orthogonal transform does not change the distribution of \mathbf{Z}_n , we have:

$$\mathbf{Z}_n^T \tilde{D}_n \mathbf{Z}_n = \mathbf{Z}_n^T Q_n^T \Lambda(\tilde{D}_n) Q_n \mathbf{Z}_n \stackrel{d}{=} \mathbf{Z}_n^T \Lambda(\tilde{D}_n) \mathbf{Z}_n = \sum_{j=1}^{3n-2} Z_{n,j}^2 \lambda_{n,j}$$

The estimation of eigenvalues of \tilde{D}_n shows that we can choose $n^{-1/2} \max_k |\lambda_k(\tilde{D}_n)| < 1/2$ for all $n \geq n_0$. To have $M_{\mathbf{Y}_n}(\lambda)$ well defined, we assume that all n in the sequel satisfy this condition.

Now, the moment-generating function $M_{\mathbf{Y}_n}(\lambda)$ we can be rewritten as:

$$M_{\mathbf{Y}_n}(\lambda) = \exp\left(-\frac{E \mathbf{G}_n^T D_n \mathbf{G}_n}{\sqrt{n}}\right) E \left[\exp\left(\sum_{j=1}^{3n-2} Z_{n,j}^2 \frac{\lambda_{n,j}}{\sqrt{n}}\right) \right]$$

Thus:

$$\begin{aligned} M_{\mathbf{Y}_n}(\lambda) &= \exp\left(-\frac{E \mathbf{G}_n^T D_n \mathbf{G}_n}{\sqrt{n}}\right) \prod_{j=1}^{3n-2} M_{\chi^2(1)}\left(\frac{\lambda_{n,j}}{\sqrt{n}}\right) \\ &= \exp\left(-\frac{E \mathbf{G}_n^T D_n \mathbf{G}_n}{\sqrt{n}}\right) \left(\prod_{j=1}^{3n-2} \frac{1}{1 - 2 \frac{\lambda_{n,j}}{\sqrt{n}}} \right)^{\frac{1}{2}} \\ &= \exp\left(-\frac{E \mathbf{G}_n^T D_n \mathbf{G}_n}{\sqrt{n}} - \frac{1}{2} \sum_{j=1}^{3n-2} \log\left(1 - 2 \frac{\lambda_{n,j}}{\sqrt{n}}\right)\right) \end{aligned}$$

By Maclaurin’s expansion:

$$\log(1 - x) = -x - \frac{x^2}{2} - \frac{x^3}{3} + o(x^3), x \rightarrow 0$$

Since $\max_{n,j} |\lambda_{n,j}|$ is uniformly bounded and $\sum_{j=1}^{3n-2} \lambda_{n,j} = \text{tr}(\tilde{D}_n) = E(Z_n^T \tilde{D}_n Z_n) = E(G_n^T D_n G_n)$, we can rewrite the expression for $M_{Y_n}(\lambda)$ as follows

$$\begin{aligned} M_{Y_n}(\lambda) &= \exp \left\{ -\frac{EG_n^T D_n G_n}{\sqrt{n}} + \frac{1}{2} \sum_{j=1}^{3n-2} \left(2\frac{\lambda_{n,j}}{\sqrt{n}} + 4\frac{\lambda_{n,j}^2}{2n} \right) + O\left(\frac{1}{\sqrt{n}}\right) \right\} \\ &= \exp \left\{ \frac{1}{n} \sum_{j=1}^{3n-2} \lambda_{n,j}^2 \right\} \exp \left\{ O\left(\frac{1}{\sqrt{n}}\right) \right\} \end{aligned}$$

Therefore, we can compute the limiting value of the first multiplier. By \tilde{D}_n , definition:

$$\begin{aligned} \sum_{j=1}^{3n-2} \lambda_{n,j}^2 &= \text{tr}(\tilde{D}_n^2) = \text{tr}((\sqrt{\Sigma_{G_n}})^T D_n \sqrt{\Sigma_{G_n}})^2 = \text{tr}((D_n \Sigma_{G_n})^2) \\ &= \sum_{i=1}^{3n-2} \sum_{j=1}^{3n-2} (D_n \Sigma_{G_n})_{ij} (D_n \Sigma_{G_n})_{ji}. \end{aligned}$$

Note that equation above may be rearranged in the following way:

$$\begin{aligned} \sum_{i=1}^{3n-2} \sum_{j=1}^{3n-2} (D_n \Sigma_{G_n})_{ij} (D_n \Sigma_{G_n})_{ji} &= \frac{\lambda_1^2}{(4-2^{2H})^2} \sum_{i=1}^{n-1} \sum_{j=1}^{n-1} \hat{\rho}_H^2(i-j) + \frac{\lambda_1 \lambda_2}{(4-2^{2H})^2} \sum_{i=1}^{n-1} \sum_{j=n}^{2n-1} \tilde{\rho}_H(j,k) \\ &+ \frac{\lambda_2^2}{4(4-2^{2H})^2} \sum_{i=1}^{2n-1} \sum_{j=1}^n \hat{\rho}_H^2(i-j) = \sum_{k=1}^3 I_n^{(k)}. \end{aligned}$$

Therefore, to obtain a limiting expression for $M_{Y_n}(\lambda)$ it suffices to divide each sum by n and to calculate the corresponding limits. A standard calculation shows:

$$\begin{aligned} \frac{1}{n(4-2^{2H})^2} \sum_{i=1}^{n-1} \sum_{j=1}^{n-1} \hat{\rho}^2(i-j) &\rightarrow 1 + \frac{2}{(4-2^{2H})^2} \sum_{i=1}^{\infty} \hat{\rho}^2(k). \\ \frac{1}{n} \frac{1}{(4-2^{2H})^2} \sum_{j=1}^{n-1} \sum_{k=1}^{2n-1} \tilde{\rho}_H^2(j,k) &\rightarrow \frac{1}{(4-2^{2H})^2} \sum_{m \in \mathbb{Z}} \tilde{\rho}_H^2(m). \end{aligned}$$

Results obtained above imply that $M(\lambda) = \exp\left\{\frac{1}{2}\lambda^T \Sigma_H \lambda\right\}$. Thus:

$$\sqrt{n} \begin{pmatrix} n^{-1}(V_{n,T}^{\hat{B}^H} - EV_{n,T}^{\hat{B}^H}) \\ (2n)^{-1}(V_{2n,T}^{\hat{B}^H} - EV_{2n,T}^{\hat{B}^H}) \end{pmatrix} \xrightarrow{d} \mathcal{N}(0; \Sigma_H)$$

Application of Slutsky’s theorem provides the required result. \square

Theorem 2. Let

$$\hat{H}_n = \frac{1}{2} - \frac{1}{2 \log 2} \log \left(\frac{\sum_{k=1}^{2n-1} (\Delta_{2n,k}^{(2)} X)^2}{\sum_{k=1}^{n-1} (\Delta_{n,k}^{(2)} X)^2} \right) \tag{10}$$

Then we can see that as $n \rightarrow \infty$, $\hat{H}_n \rightarrow H$

Moreover, we have:

$$2 \log 2\sqrt{n}(\hat{H}_n^{(1)} - H) \xrightarrow{d} N(0, \sigma_H^2)$$

where

$$\sigma_H^2 = \frac{3}{2}\Sigma_{11} - 2\Sigma_{12} \tag{11}$$

Proof. The estimator \hat{H}_n can be rewritten as:

$$\begin{aligned} \hat{H}_n &= \frac{1}{2} - \frac{1}{2\log 2} [(2H - 1) \log \frac{1}{2} + \log \frac{(\frac{2n}{T})^{2H-1} V_{2n,T}^{(2)X}}{(\frac{n}{T})^{2H-1} V_{n,T}^{(2)X}}] \\ &= H - \frac{1}{2\log 2} \log \frac{(\frac{2n}{T})^{2H-1} V_{2n,T}^{(2)X}}{(\frac{n}{T})^{2H-1} V_{n,T}^{(2)X}}, \end{aligned}$$

Using Theorem 1, the property of fractal Ornstein-Uhlenbeck and the Delta method, we can obtain:

$$2 \log 2\sqrt{n}(\hat{H}_n^{(1)} - H) \xrightarrow{d} \mathcal{N}(0, \sigma_H^2), \sigma_H^2 = \frac{3}{2}\Sigma_{11} - 2\Sigma_{12}$$

$$\Sigma_{11} = 2(1 + \frac{2}{(4 - 2^{2H})^2} \sum_{j=1}^{\infty} \hat{\rho}_H^2(j)), \Sigma_{22} = \frac{1}{2}\Sigma_{11}$$

$$\Sigma_{12} = \Sigma_{21} = \frac{1}{2^{2H}(4 - 2^{2H})^2} \sum_{j \in \mathbb{Z}} \tilde{\rho}_H^2(j)$$

$$\hat{\rho}_H(j) = \frac{1}{2}[-6|j|^{2H} - |j - 2|^{2H} - |j + 2|^{2H} + 4|j - 1|^{2H} + 4|j + 1|^{2H}],$$

$$\tilde{\rho}_H(j) = \frac{1}{2}[|j + 1|^{2H} + 2|j + 2|^{2H} - |j + 3|^{2H} + |j - 1|^{2H} - 4|j|^{2H} - |j - 3|^{2H} + 2|j - 2|^{2H}]$$

□

3.2. Alternative Estimators for the Hurst Parameter

3.2.1. MF-DFA

In this subsection we introduce two different methods for estimating the Hurst exponent, as extracted from Kantelhardt et al. [30] and Gatheral et al. [13]. The first method is the MF-DFA proposed by Kantelhardt et al. [30] and allows multi-fractality. The MF-DFA has become a popular method to study the multi-fractal properties of various time series in finance since it may be applied to non-stationary time series. The second is the qth-order SF proposed by Gatheral et al. [13].

Let us consider the time series $x_i : i = 1, 2, \dots, N$. Then, the MF-DFA involves the following five steps (most of the following algorithm is extracted from Kantelhardt et al. [30]):

(i) Compute the profile $Y(i)$ as follows:

$$Y(i) = \sum_{j=1}^i (x_j - \bar{x})$$

where \bar{x} denotes the mean of x_i for the whole sample. Therefore, the profile $Y(i)$ is the cumulative sum of the return deviations from the sample mean.

(ii) Divide the profile $Y(i)$ into $N_s = \text{int}(\frac{N}{s})$ non-overlapping segments of equal length s , where s is referred to as the time scale. Since the length N of the series is often not

a multiple of the considered time scale s , a short part at the end of the profile may remain. In order not to disregard the short part at the end of the profile when N is not a multiple of s , the same procedure is repeated starting from the opposite end. Therefore, there will be $2Ns$ segments for a given time scale s . It is recommended that the value of the time scale, s , should satisfy $10 < s < \frac{N}{4}$.

(iii) Calculate the local trend for each of the $2Ns$ segments by a least-square fit of the series. Then determine the following variance $F^2(v, s)$:

$$F^2(v, s) \equiv \frac{1}{s} \sum_{i=1}^s \{Y[(v - 1)s + i] - y_v(i)\}^2$$

For $v = Ns + 1, Ns + 2, \dots, 2Ns$. Here, $y_v(i)$ is the fitting polynomial in segment v . The fitting polynomial captures the local trend. For example, let us consider segment v that is part of the first Ns segments. This segment includes the profiles $Y[(v - 1)s + i]$, $i = 1, 2, 3 \dots, s$. The local trend of the profile for the segment can be captured by fitting the following m -order polynomial:

$$Y[t] = \alpha + \beta_1 t + \beta_2 t^2 + \dots + \beta_m t^m + \epsilon, t = (v - 1)s + 1, \dots, vs + 1$$

Then, the fitting polynomial value $y_v(i)$ is given by:

$$y_v(i) = \hat{\alpha} + \hat{\beta}_1 t + \hat{\beta}_2 t^2 + \dots + \hat{\beta}_m t^m$$

where a “hat” above the parameters indicates the estimates obtained using the ordinary least squares method. In this study, we use the first-order polynomial.

(iv) Average over all segments to obtain the q -th order fluctuation function as follows $q \neq 0$:

$$F_q(s) \equiv \left\{ \frac{1}{2Ns} \sum_{v=1}^{2Ns} [F^2(v, s)]^{q/2} \right\}^{1/q}$$

The q -th order fluctuations are similar to q -th order moments. However, in the MF-DFA, q can take negative values. The main purpose of using q -th order fluctuation has to do with the power-law, mentioned in the next step, which allows us to distinguish a multi-fractal model from a mono-fractal model. We are interested in how the generalized q dependent fluctuation functions $F_q(s)$ depend on the time scale s for different values of q . Hence, we must repeat steps 2 to 4 for several time scales, s . It is apparent that $F_q(s)$ will increase with increasing s . Of course, $F_q(s)$ depends on the DFA order m . By construction, $F_q(s)$ is only defined for $s \geq m + 2$.

(v) Determine the scaling behavior of the fluctuation functions by analyzing log-log plots $F_q(s)$ versus s for each value of q . If the series x_i are long-range power-law correlated, $F_q(s)$ increases, for large values of s , as a power-law:

$$F_q(s) \sim s^{h(q)}$$

It is clear from the equation above that $F_0(s) = \lim_{q \rightarrow 0} F_q(s)$ and, therefore, $h(0) = \lim_{q \rightarrow 0} h(q)$, cannot be determined using the averaging procedure. Therefore, for $q = 0$, a logarithmic averaging procedure is employed as follows:

$$F_0(s) \equiv \exp \left\{ \frac{1}{4Ns} \sum_{v=1}^{2Ns} \ln F^2(v, s) \right\} \sim s^{h(0)}$$

For each q (referred to as moment order), perform a linear regression of $\ln F_q(s)$ on $\ln(s)$ for all s . The slope of the regression will be the estimator of the generalized Hurst exponent $h(q)$.

3.2.2. The qth-Order SF Method

We also determined $h(q)$ from the qth-order SF method used in Gatheral et al. [13]. In the spirit of Gatheral et al. [13], we assume that discrete observations of the spot volatility process, on a time grid with mesh Δ on $[0, T]$ are $\sigma_0, \sigma_\Delta, \dots, \sigma_{k\Delta}, \dots, k \in \{0, \lfloor T/\Delta \rfloor\}$. Set $N = \lfloor T/\Delta \rfloor$, then for $q \geq 0$, we can define

$$m(q, \Delta) = \frac{1}{N} \sum_{k=1}^N \left| \log(\sigma_{k\Delta}) - \log(\sigma_{(k-1)\Delta}) \right|^q$$

Under the assumption that the log-spot-volatility process is stationary and that a law of large numbers holds, for some values of q we can see that qH has monofractal scaling properties which imply that

$$m(q, \Delta) \sim C\Delta^{qH}$$

As Δ tends to zero and with constant of proportionality C .

Let $\beta_1 = \log K_q$. We further use the market data via the regression

$$\log(m(q, \Delta)) = \beta_1 + \beta_2 \log \Delta + \epsilon \tag{12}$$

which provides an estimator:

$$H_{qSF} = \frac{\beta_2}{q} \tag{13}$$

For several orders of q , the regression of the slope in (12) against q reveals that the different orders of q lead to the same estimate of H as the one obtained when $q = 2$.

3.2.3. Two Least Square Estimation Methods

To test the roughness of the spot volatility, we must estimate the Hurst exponents. In fact, there exists a vast literature that describes different methods for estimating the Hurst parameter of the fractional Brownian motion (fBm) including parametric estimation methods, semi-parametric estimation and non-parametric estimation approaches. In this paper, we adopt two types of estimators for the Hurst parameter, which are proven to be strongly consistent and asymptotically normal.

Let $X_t = \log(\sigma_t)$ as in model (1), and denotes $M_k(n) = \frac{1}{n-1} \sum_{i=0}^{n-2} (X_{(i+2)\Delta} - 2X_{(i+1)\Delta} + X_{i\Delta})^k$, where $n \in \mathbb{N}^+ - 1, k \in \mathbb{R}^+$. The first estimator \hat{H}_k of Hurst parameter H by the least squares estimation method introduced by Berzin et al. [31], is calculated as follows

$$\begin{aligned} \hat{H}_k &= -\frac{1}{k} \sum_{i=1}^{\ell} z_i \log(M_k(n_i)) \\ &= -\frac{1}{k} \sum_{i=1}^{\ell} z_i \log\left(\frac{1}{n_i-1} \sum_{j=0}^{n_i-2} (X_{(j+2)\Delta} - 2X_{(j+1)\Delta} + X_{j\Delta})^k\right), \end{aligned} \tag{14}$$

where $n_i = r_i n, r_i \in \mathbb{N}^*, i = 1, \dots, \ell$ and $z_i = \frac{y_i}{\sum_{i=1}^{\ell} y_i^2}$ and $y_i = \log(r_i) - \frac{1}{\ell} \sum_{i=1}^{\ell} \log(r_i)$.

Let $M_{\log}(n) = \frac{1}{n-1} \sum_{i=0}^{n-2} \log(|X_{(i+2)\Delta} - 2X_{(i+1)\Delta} + X_{i\Delta}|)$. The second estimator \tilde{H}_{\log} of H derived by the least square estimation method in Berzin et al. [31] is expressed as

$$\begin{aligned} \tilde{H}_{\log} &= -\sum_{i=1}^{\ell} z_i M_{\log}(n_i) \\ &= -\sum_{i=1}^{\ell} z_i \frac{1}{n_i-1} \sum_{j=0}^{n_i-2} \log(|X_{(j+2)\Delta} - 2X_{(j+1)\Delta} + X_{j\Delta}|). \end{aligned} \tag{15}$$

The estimator \hat{H}_k is an asymptotically unbiased strongly consistent estimator of H , and the estimator \hat{H}_{\log} is an unbiased weakly consistent estimator of H . The asymptotic distribution of estimators \hat{H}_k and \hat{H}_{\log} can be found in Berzin et al. [31].

From remark 3.12 and remark 3.15 of Berzin et al. [31], asymptotic theory for \hat{H}_k and \hat{H}_{\log} there is a corollary. The estimator \hat{H}_k is an asymptotically unbiased strongly consistent estimator of H and the estimator \hat{H}_{\log} is an unbiased weakly consistent estimator of H . Furthermore, for $k = 2r_i = 2^{i-1}$ and $i = 1, \dots, \ell$, we have:

$$\begin{aligned} \sqrt{n}(\hat{H}_k - H) &\xrightarrow{d} \mathcal{N}\left(0, \sigma_{\hat{H}_k}^2\right) \\ \sqrt{n}(\hat{H}_{\log} - H) &\xrightarrow{d} \mathcal{N}\left(0, \sigma_{\hat{H}_{\log}}^2\right) \end{aligned}$$

where

$$\sigma_{\hat{H}_k}^2 = \left(\frac{6}{\log(2)}\right)^2 \frac{1}{\ell^2(\ell-1)^2} \times \left(2 \sum_{i < j, i, j=1}^{\ell} 2^{-j}(2i - (\ell + 1))(2j - (\ell + 1)) \times \sum_{r=-\infty}^{+\infty} \rho_{1,2^j-i}^2(r) + \sum_{i=1}^{\ell} 2^{-i}(2i - (\ell + 1))^2 \sum_{r=-\infty}^{+\infty} \rho_H^2(r)\right) \tag{16}$$

$$\begin{aligned} \sigma_{\hat{H}_{\log}}^2 &= \left(\frac{3}{\log(2)}\right)^2 \frac{1}{\ell^2(\ell-1)^2} \left(2 \sum_{i < j, i, j=1}^{\ell} 2^{-j+1}(2i - (\ell + 1))(2j - (\ell + 1)) \right. \\ &\times \sum_{p=1}^{+\infty} (2p)! \left(\frac{1}{p(2p-1)!!}\right)^2 \sum_{r=-\infty}^{+\infty} \rho_{1,2^j-i}^{2p}(r) + \sum_{i=1}^{\ell} 2^{-i+1}(2i - (\ell + 1))^2 \\ &\times \sum_{p=1}^{+\infty} (2p)! \left(\frac{1}{p(2p-1)!!}\right)^2 \sum_{r=-\infty}^{+\infty} \rho_H^{2p}(r) \left. \right) \end{aligned} \tag{17}$$

$$\begin{aligned} \rho_{b,c}(x) &= \frac{1}{2(4-2^{2H})} (bc)^{-H} [-|x|^{2H} + 2|x-b|^{2H} - |x-2b|^{2H} \\ &+ 2|x+c|^{2H} - 4|x+c-b|_{2H} + 2|x+c-2b|_{2H} - |x+2c|_{2H} \\ &+ 2|x+2c-b|_{2H} - |x+2c-2b|_{2H}] \\ \rho_H(x) &= \frac{-6|x|^{2H} + 4|x+1|^{2H} - |x+2|^{2H} - |x-2|^{2H} + 4|x-1|^{2H}}{2(4-2^{2H})} \end{aligned}$$

3.3. Comparison of Asymptotic Variance of H_k , H_{\log} and H_n

In this subsection, we compare Hurst exponents according to the three variance Formulas (11), (16) and (17). Although, in theory, H_k , H_{\log} and H_n can eventually converge to the true value, in engineering practice, the value of ℓ , p, r cannot be very large, which means that there must be errors in the three Hurst exponent estimates under the condition of limited computing resources. Therefore, we try to compare the advantages and disadvantages of the three according to the asymptotic variance under different parameter values.

As can be seen from Table 1, with the increase in the number of ℓ , \hat{H}_k and \hat{H}_{\log} have a downward trend, but overall, the asymptotic variance of \hat{H}_k is less than \hat{H}_{\log} . From this point of view, \hat{H}_k is a better estimate.

Table 1. Comparison of asymptotic variance of H_k and H_{log} .

H	ℓ	0.1	0.2	0.3	0.4	0.5	0.6	0.7	0.8	0.9
\hat{H}_k	2	61.43384	60.09544	58.74345	57.42546	56.19696	55.12336	54.28286	53.77096	53.7078
	5	9.179444	9.099669	8.987028	8.86357	8.745652	8.646854	8.57992	8.558286	8.597588
	10	2.973535	2.891396	2.820534	2.762025	2.716779	2.686191	2.672437	2.678699	2.709498
\hat{H}_{log}	2	165.8243	75.86426	74.52995	73.18453	71.87646	70.66238	69.6092	68.7972	68.32469
	5	11.05752	10.97854	10.86696	10.74497	10.62911	10.53315	10.47013	10.45383	10.50042
	10	3.51451	3.432525	3.361931	3.303832	3.259175	3.229411	3.216792	3.22461	3.257532

According to Figure 1 and Table 1, H_k is usually better than H_{log} when the parameter ℓ has a limited value. The variance of H_k is small, but H_{log} converges slightly faster with an increase of ℓ . In general, H_k is recommended in practice.

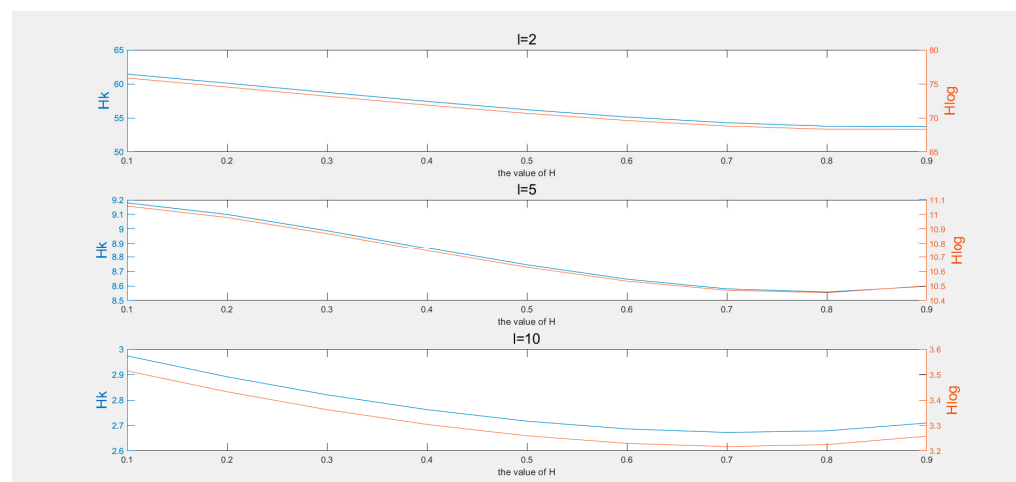


Figure 1. Comparison of asymptotic variance of H_k and H_{log} .

Next, given $\ell = 10$, compare the asymptotic variance of H_n with that of H_k and H_{log} . Table 2 shows the change of H values from 0.1 to 1. It can be seen that as the value of H increases, the error of H_n becomes smaller and smaller. When $H > 0.4$, the asymptotic variance of H_n is smaller than H_k and H_{log} .

Table 2. Comparison of asymptotic variance of H_n with H_k and H_{log} .

$\ell=10$.										
H	0.1	0.2	0.3	0.4	0.5	0.6	0.7	0.8	0.9	
\hat{H}_k	2.973535	2.891396	2.820534	2.762025	2.716779	2.686191	2.672437	2.678699	2.709498	404
\hat{H}_{log}	3.51451	3.432525	3.361931	3.303832	3.259175	3.229411	3.216792	3.22461	3.257531	1806
\hat{H}_n	4.055571	3.812466	3.552612	3.280313	3	2.716159	2.433252	2.155608	1.887306	706

A similar situation is shown in Figure 2. H_n decreases as the value of H increases; after 0.4, the asymptotic variance of H_n is less than that of H_k and H_{log} .

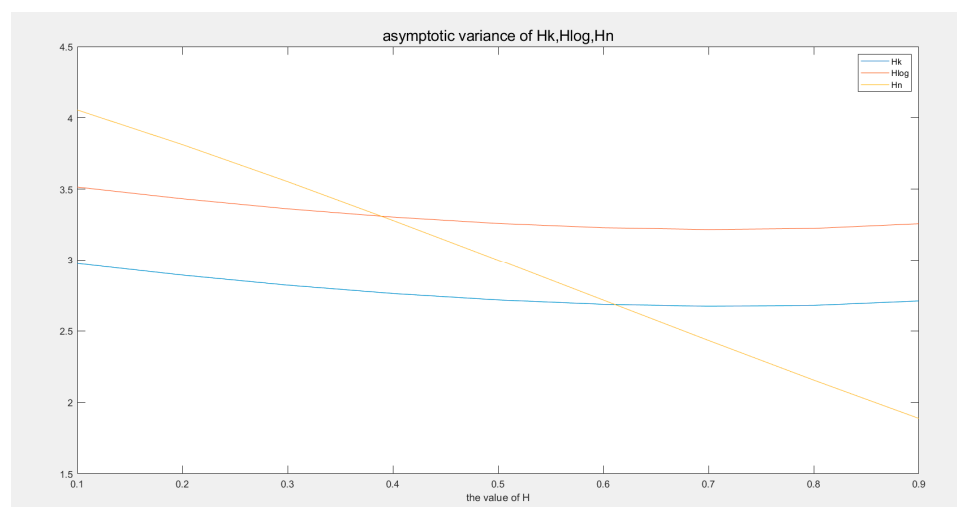


Figure 2. Comparison of asymptotic variance of H_n with that of H_k and H_{log} .

4. Research on the Roughness of Truncated and Non-Truncated Spot Volatility of Chinese A-Share Industry Indices Estimated by Five Hurst Exponents

4.1. Data Description

We collected Shanghai Composite Index and Shanghai Industrial Index series data from the WIND High-frequency database. The sampling frequency was set at 5 min, which allowed us to circumvent all the issues associated with micro-structure noise and thereby focus on questions pertinent to this paper. For assets in the Chinese stock market, we considered the Shanghai Composite Index (also named SSE Index), the most influential index in China's capital market, and the Shanghai Industrial Index series consisting of 10 primary industries.

The Shanghai Composite Index, published on 15 July 1991, is the first flagship index reflecting the overall market trend in Shanghai. It includes all the stocks listed on the Shanghai Stock Exchange, such as A shares and B shares, and is weighted by the total share capital, representing the 30-year development process of China's capital market. It is a symbol of China's capital market. The data set at our disposal ran from 1 January 2005 until 31 December 2020. We excluded weekends and holidays and kept only full trading days, which resulted in 3888 days. Thus, we obtained 48 observations for every trading day and obtained 186,624 observations for the SSE index. According to industry classification standards, the Shanghai Industrial Index series consists of 10 primary industries, such as the Energy Sector (SSE Energy), Raw Materials Sector (SSE Materials), Industrials Sector (SSE Industrials), Consumer Discretionary Sector (SSE ConsDisc), Consumer Staples Sector (SSE ConsStaples), Health Care Sector (SSE HealthCare), Financials Sector (SSE Financials), Information Technology Sector (SSE InfoTechnology), Telecommunication Services Sector (SSE TelecomSvc), and the Utilities Sector (SSE Utilities), which cover almost all samples of the Shanghai stock market and represent the development process of the relating industries. A detailed descriptions and interpretations for the ten indices are as follows:

1. Base date and base index. The base date of the Shanghai stock exchange industry index series is 9 January 2009, and the base index is 1000.
2. Index sample stocks selection. The sample stock space of series of the Shanghai industry index is composed of all sample stocks of Shanghai Index. Based on the international mainstream industry classification standards and the characteristics of China's listed companies, the listed companies are divided into 10 industries: energy, raw materials, industry, optional consumption, main consumption, medicine and health, finance and real estate, information technology, telecommunication business and public utilities.
3. Sample stock selection method. The stocks in the sample space are classified according to the industry classification standard, and all the stocks in their respective industries constitute the sample stocks of the corresponding industry index.

4. Index calculation and correction. The industry index series of Shanghai stock exchange adopts the Paasehe weighting method, and the weighted calculation formula is as follows.

Index in the reporting period = adjusted market value of sample stock in the reporting period/base period × 1000.

Specifically, adjust market value = stock price × adjusted capital stock. The adjusted capital stock is the capital stock after adjusting the capital stock of the sample stock by “grading and classifying”.

5. Sample stock adjustment. When the Shanghai Stock Index adjusts the sample stocks, the industry index series of Shanghai stock index is adjusted accordingly. When the sample company has a special event, which leads to the change of its industry ownership, the sample stock of Shanghai stock exchange industry index series is adjusted accordingly.

The data set at our disposal run from 1 January 2010 until 31 December 2020, which results in 2673 days by keeping only full trading days. Thus, we obtain 48 observations for every trading day and obtain 128,304 observations for each industrial index.

4.2. Non-Truncated Spot Volatility

Ignoring the effects of jumps in the prices, we can apply the non-truncated estimator of Equation (2) to extract spot volatilities using the 5 min high-frequency data. The estimation procedure calculating with $\Delta_n = 5/240$ and $k_n = 96$ results in 1944 estimates of non-truncated spot volatility for the SSE Index and 1337 estimates of non-truncated spot volatilities for each industrial index. To give a brief insight into the properties of the 11 indices, Table 3 reports summary statistics for non-truncated spot volatility, where Std.Dev denotes standard derivation. Index abbreviations are given in the first column. The second to sixth columns contain some basic descriptive statistics for the indices, including the mean, minimal, median, maximal and standard deviation of the spot volatility estimates. Moreover, both skewness and kurtosis are presented in the last two columns of Table 3.

Table 3. Descriptive statistics for the non-truncated spot volatility and its logarithm.

stat_non_trunc	Mean	Min	Max	Median	Std.Dev	Skewness	Kurtosis
Panel A: Non-truncated Spot Volatility							
SSE index	0.00022	9.05×10^{-6}	0.00484	0.00010	0.00037	5.61360960	47.7565
SSE Energy	0.00025	1.48×10^{-5}	0.00613	0.00014	0.00045	6.96110970	69.8107
SSE Materials	0.00026	1.74×10^{-5}	0.00810	0.00014	0.00051	8.30235757	95.8771
SSE Industrials	0.00023	1.02×10^{-5}	0.00787	0.00010	0.00052	8.19252067	90.0560
SSE Cons Disc	0.00021	9.85×10^{-6}	0.00648	0.00011	0.00041	8.81983563	106.233
SSE Cons Staples	0.00020	1.14×10^{-5}	0.00659	0.00012	0.00037	9.56348181	128.357
SSE Health Care	0.00019	7.73×10^{-6}	0.00603	0.00011	0.00035	8.82946172	113.921
SSE Financials	0.00021	1.04×10^{-5}	0.00562	0.00011	0.00038	6.87344218	67.1841
SSE Info Technology	0.00031	2.28×10^{-5}	0.00727	0.00018	0.00048	7.08361470	76.6140
SSE Telecom Svc	0.00034	2.38×10^{-5}	0.00934	0.00018	0.00061	7.56650831	79.6772
SSE Utilities	0.00017	1.13×10^{-5}	0.00587	7.65×10^{-5}	0.00040	7.96280129	83.3764
Panel B: Logarithm of non-truncated spot volatilities							
SSE index	-9.0228	-11.6127	-5.3299	-9.1544	1.04418	0.48284956	2.92738
SSE Energy	-8.8034	-11.1212	-5.0932	-8.8651	0.93912	0.56099374	3.72217
SSE Materials	-8.7734	-10.959	-4.8149	-8.8504	0.92463	0.64137993	3.95554
SSE Industrials	-9.0030	-11.4906	-4.8435	-9.1269	0.95747	0.87836819	4.56345
SSE Cons Disc	-8.9992	-11.5282	-5.0387	-9.0412	0.92581	0.50655449	4.08381
SSE Cons Staples	-8.9353	-11.3815	-5.0212	-8.9969	0.82634	0.65934088	4.71016
SSE Health Care	-9.0657	-11.7707	-5.11096	-9.0936	0.94631	0.29717300	3.91282
SSE Financials	-8.9995	-11.4702	-5.1811	-9.0533	0.96055	0.43924226	3.75374
SSE Info Technology	-8.4958	-10.689	-4.9236	-8.5761	0.87165	0.45663801	3.65189
SSE Telecom Svc	-8.4808	-10.645	-4.6731	-8.5727	0.86341	0.78021763	4.49018
SSE Utilities	-9.3710	-11.3898	-5.1368	-9.4783	0.98057	0.94548892	4.67285

Panel A of Table 3 shows that mean values of the non-truncated spot volatility range from 0.0002 to 0.0003 for all indices. SSE TelecomSvc displays the highest standard deviation (i.e., 0.00061). Considering skewness and kurtosis, the SSE Index achieves the lowest values while the highest values are obtained for SSE ConsStaples. None of the series seems to be symmetric. Moreover, all the time series have positive skewness, which implies that the distributions have a long right tail.

As stated in Da Fonseca and Zhang [21], taking the logarithm has the well-known effect of reducing the discrepancies between variables and makes distributions closer to normal distributions. Panel B of Table 3 shows that skewness of the logarithm of non-truncated spot volatilities are much smaller, and the kurtosis are closer or a little bigger than 3.

The main reason for positive skewness and high kurtosis might be comprised of the effect of jumps which we don't filter in the data. Therefore, we next considered the case when there are jumps in the asset prices.

4.3. Truncated Spot Volatility

To consider the effect of jumps, we estimate the spot volatility using the truncated estimator of Equation (3) with $k_n = 96$, $\Delta_n = 5/240$ and $v_n = \sqrt{\Delta_n/250}$. Table 4 provides the basic descriptive statistics for the truncated spot volatility. As shown in Panel A of Table 4, the mean values and standard deviations of the truncated spot volatility indexes are all around 0.0001–0.0002. These positive values for the skewness of the spot volatility indexes indicate that all the spot volatility indexes are skewed right. The values for the kurtosis of the spot volatility indexes are always greater than 3, which indicates a heavy-tailed distribution. By taking the logarithm, Panel B of Table 4 shows that the skewness of the logarithm of truncated spot volatility of all the indices are near the expected value of zero, and the kurtosis of the logarithm of truncated spot volatility of all the indices are near the expected value of 3. Hence, the values of skewness and kurtosis of the logarithm of truncated spot volatility indexes are acceptable ranges for being normally distributed, which would make the Hurst parameter estimators maintain their good properties.

4.4. Hurst Exponent Estimation

By using the derived logarithm of non-truncated and truncated spot volatility series of the Composite Index and the 10 industrial indices data in the Chinese stock market, we calculated the Hurst parameter using the four Hurst parameter estimators, $H_n, H_k, H_{log}, H_{qSF}$ in Section 2.

When we calculate the estimator H_{qSF} from (13) by the q th-order SF method, we should refine how the regression slope β_2 from regression (12) depends on the order q . By the mono-fractal scaling properties, we suppose $\beta_2 \sim Hq$, which leads us to a similar estimate of the Hurst exponent by (13).

By taking $q = 1, 1.5, 2, 2.5, 3, 3.5$ and conducting a linear regression of (12) for $\Delta = 1, 2, 3, \dots, 100$, Figure 3 shows the linear relationship of β_2 and q based on logarithm forms of both non-truncated spot volatility and truncated spot volatility for the Shanghai Composite Index (SSE Index). Additional test results for the 10 industrial indices are shown in Figures 4 and 5. All the figures illustrate the approximate linear relationship between β_2 and q , which is consistent with the theoretical derivation in Gatheral et al. [13] and lead us to a similar estimate of the Hurst parameter by (13).

Table 4. Descriptive statistics for the truncated spot volatilities and their logarithms.

stat_trunc	Mean	Min	Max	Median	Std.Dev	Skewness	Kurtosis
Panel A: Truncated spot volatilities							
SSE index	0.00015	9.05×10^{-6}	0.00093	9.38×10^{-5}	0.00015	1.910627	6.71405
SSE Energy	0.00016	1.48×10^{-5}	0.00089	0.00011	0.00014	2.162615	8.26727
SSE Materials	0.00016	1.74×10^{-5}	0.00082	0.00012	0.00014	2.072311	7.87712
SSE Industrials	0.00014	1.02×10^{-5}	0.00090	0.0001	0.00013	2.476477	9.72460
SSE Cons Disc	0.00013	9.85×10^{-6}	0.00077	0.00010	0.00011	2.323363	9.81297
SSE Cons Staples	0.00014	1.14×10^{-5}	0.00081	0.00011	0.00010	2.505865	11.2342
SSE Health Care	0.00013	7.73×10^{-6}	0.00085	0.00010	0.00011	2.366167	10.4674
SSE Financials	0.00014	1.04×10^{-5}	0.00102	0.00010	0.00013	2.684608	12.6908
SSE Info Technology	0.00021	2.28×10^{-5}	0.00095	0.00016	0.00015	1.64547	5.96398
SSE Telecom Svc	0.00020	2.38×10^{-5}	0.00100	0.00016	0.00014	1.889841	7.25645
SSE Utilities	0.00010	1.01×10^{-5}	0.00086	7.26×10^{-5}	0.00012	3.081249	13.9049
Panel B: Logarithm of truncated spot volatilities							
SSE index	-9.1803	-11.612	-6.9750	-9.2744	0.88871	0.197569	2.41616
SSE Energy	-9.0321	-11.121	-7.0142	-9.0610	0.76953	0.124777	2.77233
SSE Materials	-8.9674	-10.959	-7.1063	-8.9712	0.74074	0.099774	2.73774
SSE Industrials	-9.1668	-11.490	-7.0048	-9.2100	0.76706	0.275856	3.15982
SSE Cons Disc	-9.1697	-11.528	-7.1616	-9.1632	0.76327	-0.04621	3.00242
SSE Cons Staples	-9.0922	-11.381	-7.1069	-9.1035	0.66098	0.002958	3.49107
SSE Health Care	-9.2145	-11.770	-7.069	-9.1831	0.78518	-0.28041	3.35773
SSE Financials	-9.1818	-11.470	-6.8844	-9.2013	0.79877	-0.00218	3.09299
SSE Info Technology	-8.6952	-10.689	-6.9569	-8.7076	0.6935	-0.10739	2.91148
SSE Telecom Svc	-8.6995	-10.645	-6.9032	-8.7227	0.65081	0.013933	3.01487
SSE Utilities	-9.4973	-11.507	-7.0505	-9.5307	0.8180	0.394645	3.19111

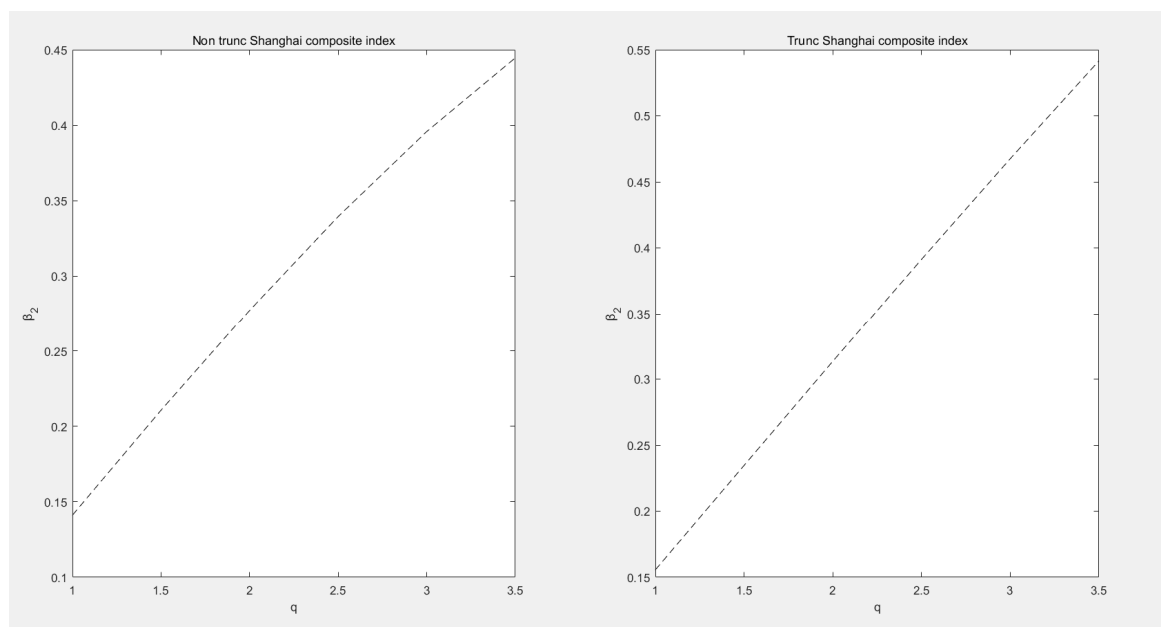


Figure 3. β_2 against q based on logarithm forms of both non-truncated spot volatility and truncated spot volatility for the Shanghai Composite Index (SSE Index).

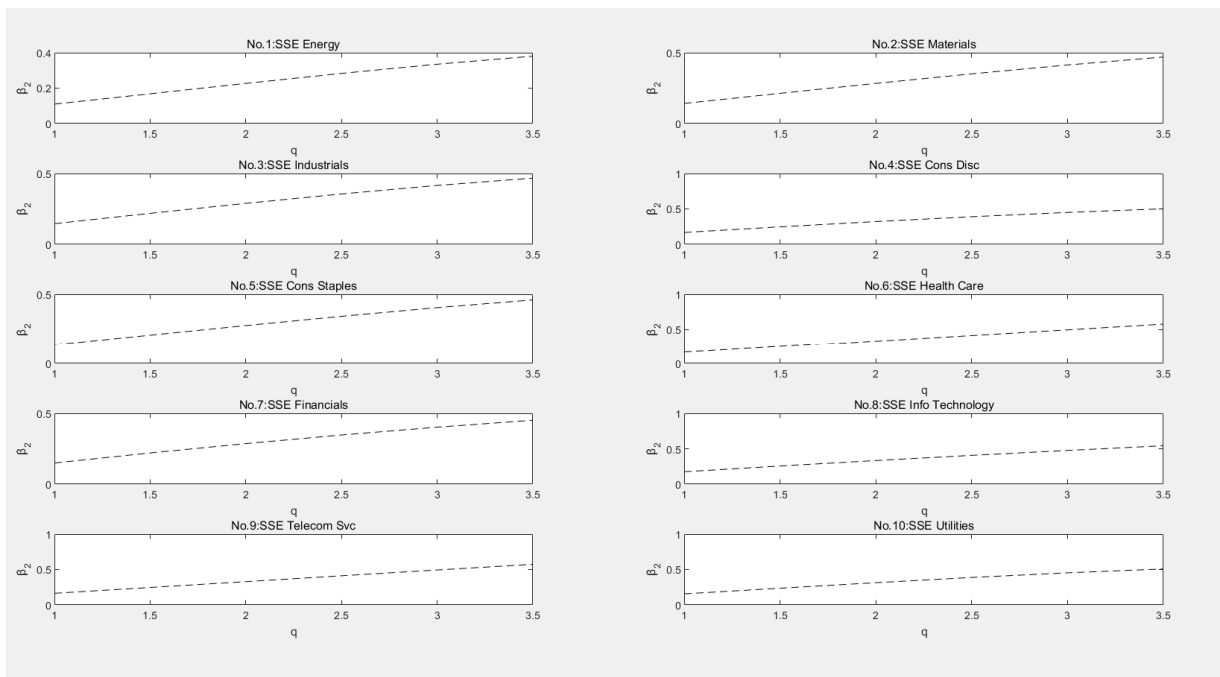


Figure 4. β_2 against q based on the logarithm of non-truncated spot volatility for the 10 industrial indices.

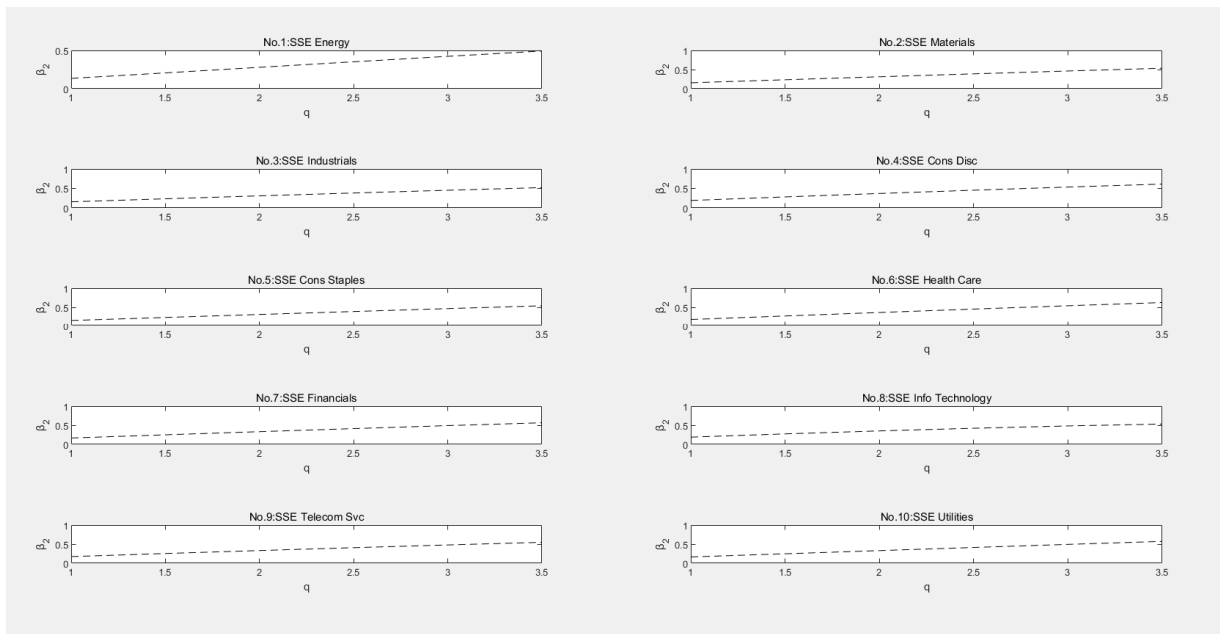


Figure 5. β_2 against q based on the logarithm of truncated spot volatility for the 10 industrial indices.

For all the indices, we can calculate the Hurst exponents by the five different Hurst exponent estimators using both non-truncated spot volatility and truncated spot volatility in logarithm forms. From the Hurst exponent estimation results listed in Table 5, we can see the Hurst exponents are all less than 0.5 for all the indices, no matter which Hurst exponent estimator we adopt, and whether or not price jumps are filtered. The results in Table 5 indicate the roughness in the log-volatility of the Composite Index and the 10 industrial indices in the Chinese stock market, consistent with findings in the literature, such as Gatheral et al. [13], Livieri et al. [14], Da Fonseca and Zhang [21] and Takaishi [23]; Bennedsen et al. [11]. Our study provides further evidence of the roughness in spot volatility.

Table 5. Hurst parameter estimates for the logarithm of spot volatilities.

Index	Log (Non-Truncated Spot Volatility)					Log (Truncated Spot Volatility)				
	H_k	H_{log}	H_{qSF}	H_n	MF-DFA	H_k	H_{log}	H_{qSF}	H_n	MF-DFA
SSE index	0.27	0.22	0.09	0.27	0.22	0.27	0.17	0.16	0.19	0.26
SSE Energy	0.33	0.28	0.06	0.33	0.23	0.33	0.22	0.05	0.24	0.26
SSE Materials	0.26	0.25	0.28	0.26	0.22	0.26	0.27	0.09	0.26	0.26
SSE Industrials	0.29	0.26	0.18	0.29	0.20	0.29	0.18	0.21	0.15	0.27
SSE Cons Disc	0.23	0.18	0.16	0.23	0.25	0.23	0.25	0.20	0.23	0.28
SSE Cons Staples	0.20	0.17	0.25	0.20	0.22	0.20	0.23	0.13	0.23	0.21
SSE Health Care	0.22	0.21	0.11	0.22	0.27	0.22	0.20	0.22	0.17	0.34
SSE Financials	0.23	0.24	0.27	0.23	0.15	0.23	0.21	0.11	0.20	0.23
SSE Info Technology	0.33	0.33	0.21	0.32	0.18	0.33	0.29	0.23	0.29	0.23
SSE Telecom Svc	0.37	0.38	0.10	0.37	0.21	0.37	0.31	0.21	0.30	0.25
SSE Utilities	0.27	0.22	0.09	0.27	0.22	0.27	0.33	0.15	0.28	0.26

5. Discussion

It is well-known that the constant volatility of Black and Scholes [1] is neither consistent with real volatility data nor consistent with implied volatility surfaces. Consequently, several popular stochastic volatility models driven by standard Brownian motions have been introduced in past decades to reproduce the stylized facts of time series observed for both the historical volatility and the implied volatility. Moreover, in order to take into account an apparent presence of long memory in the volatility process, Comte and Renault [6] first proposed a stochastic volatility model driven by fractional Brownian motion (fBm) with $H > 1/2$. Recently, prompted by new insights from realized volatility data, Gatheral et al. [13] and Bennedsen et al. [11] introduced rough volatility models driven by fBm with $H < 1/2$. Using absolute moments estimation and realized volatility as a proxy of true volatility, Gatheral et al. [13] estimate the Hurst exponent and found that it is close to 0.14 for both the log-volatility of the SP500 and the NASDAQ, together with other major indices. Moreover, the estimation of the Hurst exponent H is robust across time, scales and markets. More empirical studies of the log-volatility for thousands of stocks (see, e.g., Bennedsen et al. [11]) and implied volatility (see, e.g., Livieri et al. [14]) confirm the roughness of the volatility.

Since the spot volatility is of importance in several applications, including derivatives pricing, high-frequency trading, and risk management, it is natural to assess whether spot volatility has a rough property, that is, to determine whether the spot volatility is rough.

Many publications consider the roughness of realized volatility and implied volatility. Gatheral et al. [13] showed the volatility roughness of SP500 index, Livieri et al. [14] showed that implied volatility is rough, too. Takaishi [23] studied Bitcoin and verified the roughness of volatilities in Bitcoin. Da Fonseca and Zhang [21] found the volatility of volatility is also rough. Bennedsen et al. [11] found the roughness of logarithmic volatility of thousands of stocks. There is much evidence showing the roughness of volatility in different sectors and markets (see Guennoun et al. [32], Funahashi and Kijima [33], Neuenkirch and Shalaiko [34]). However, spot volatility is still a problem, especially the comparison of truncated and non-truncated spot volatility. This paper fills the gaps in previous works.

Following the important work of Gatheral et al. [13], this study aims to provide further evidence of the roughness of logarithm spot volatility in the Chinese financial market. Using the non-parametric estimator proposed by Fan and Wang [28], this paper introduces a non-parametric spot volatility estimator for the fractional volatility model of (1) for all $H \in (0, 1)$. Using five different Hurst exponents, MF-DFA, q th-order SF, two Hurst estimations using the least square estimation method provided by Berzin et al. [31] and a new Hurst exponent by changing frequency method, this paper analyzed roughness of the log-realized volatility of 10 industrial indices in the Chinese financial market. We found that $h(q)$ calculated by five different Hurst exponents were all less 0.5. These results confirm the roughness of log-spot volatility.

Moreover, we propose a new Hurst estimation H_n by changing the data frequency method. This performs better when $H > 0.4$ in the perspective of asymptotic variance.

6. Conclusions

Volatility is very important in many aspects of the financial field. First, implied volatility is the key in option pricing relative to the realized volatility, and a model of realized volatility can be used to improve the option pricing effectiveness. Second, volatility is a way to measure risk. With the continuous development of the financial market, financial assets such as stocks, futures, bonds and foreign exchange are constantly enriched. No matter the kind of financial asset, price risk is always one of the core risks. The most direct manifestation of the sharp rise and fall of prices is the rise of volatility, so how to measure and predict volatility is a very important problem. Therefore, modeling and prediction of volatility is the answer to the basic problem of the financial risk, and its significance is self-evident. Third, volatility is an indicator of financial supervision on micro market behavior. Financial market supervision often faces a dilemma: on the one hand, we should encourage financial innovation, but innovation often brings new problems, such as new market risks or new institutional arbitragers. On the other hand, we should not be too conservative, otherwise it is easy to suppress market vitality and solidify market ecology; then we may lose the fairness of the market. With the popularity of financial big data, regulators have more micro-detailed data, which provides the possibility for fixed-point and local supervision. So how to mine and depict the behavior of market participants from massive data is an important problem. Macro and micro financial behaviors, related to the banker, money laundering, financial crises, credit default, and so on, have effects on market price. When the market price changes dramatically, this reflects volatility. Therefore, the volatility can become a tool and a starting point for supervision in the era of financial big data.

Since volatility modelling is so important, this section summarizes the contributions of studies of roughness of volatility, which is one its most important properties. First, we propose a Hurst estimation H_n by changing the data frequency method. Second, we prove the asymptotic variance of H_n and that of two Hurst estimations provided by Berzin et al. [31], and do simulations to find the advantages of H_n that H_n that work better than those of Berzin et al. [31] when $H > 0.4$. Third, since much literature verifies the roughness of volatility (including volatility of the SP500 index by Gatheral et al. [13], implied volatility of options by Livieri et al. [13], volatility of bitcoin by Takaishi [23], volatility of volatility by Da Fonseca and Zhang [21], and volatility of many stocks by Bennedsen et al. [11]), we fill a gap that verifies the roughness of truncated and non-truncated spot volatility by four different Hurst exponent estimations: $H_n, H_k, H_{log}, H_{qSF}$. We find that truncated spot volatility has a stronger roughness than that of non-truncated spot volatility.

This study also suggests several important directions for future research. The estimator methods of constructing the estimators and their asymptotic properties essentially depend on observations. The first suggestion is to include estimation error and microstructure noise into the analysis. The second suggestion is to construct a unified volatility model that correctly accounts for, if possible, all the stylized facts observed in the real data, such as volatility clustering, multi-fractality, roughness, mean-reversion and persistence. Another direction for future research is to discuss the pricing and hedging of volatility options in some rough volatility models. In such cases, efficient Monte Carlo methods and asymptotic approximations for computing option prices and hedge ratios should be employed, which might provide insight into the robustness of the results obtained herein.

Author Contributions: Methodology, Y.L.; software, Y.L.; formal analysis, Y.L.; writing—review and editing, Y.L.; validation, Y.T.; resources, Y.T. All authors have read and agreed to the published version of the manuscript.

Funding: This research received no external funding.

Institutional Review Board Statement: The study was conducted in accordance with the Declaration of Helsinki, and approved by the Institutional Review Board.

Informed Consent Statement: Not applicable.

Data Availability Statement: The data used to support the findings of this study are available from the corresponding author upon request.

Acknowledgments: All individuals included in this section have consented to the acknowledgement.

Conflicts of Interest: The authors declare that there are no conflicts of interest regarding the publication of this paper.

Appendix A

Proof of Lemma 1. We give brief derivations here.

From (1), for all $H \in (0, 1)$, we have

$$\begin{aligned} X_t &= (1 - e^{-\alpha t})m + X_0e^{-\alpha t} + v \int_0^t e^{-\alpha(t-s)}dB_s^H \\ &= (1 - e^{-\alpha t})m + X_0e^{-\alpha t} + vB_t^H - \alpha ve^{-\alpha t} \int_0^t e^{\alpha s}B_s^H ds \\ &= (1 - e^{-\alpha t})m + X_0e^{-\alpha t} + \tilde{X} \end{aligned} \tag{A1}$$

where $\tilde{X}_t = vB_t^H - \alpha ve^{-\alpha t} \int_0^t e^{\alpha s}B_s^H ds$

Thus, \tilde{X}_t is normal distribution with mean $(1 - e^{-\alpha t})m + X_0e^{-\alpha t}$. For the sake of convenience, we first consider the covariance of \tilde{X}_t and \tilde{X}_s . Using the well known result, $R_H(s, t) = \frac{1}{2}(|t|^{2H} + |s|^{2H} - |t - s|^{2H})$, supporting $t > s > 0$, the covariance function of, \tilde{X}_t and \tilde{X}_s is given by:

$$\begin{aligned} \text{cov}(\tilde{X}_t, \tilde{X}_s) &= \mathbb{E}[(-\alpha ve^{-\alpha t} \int_0^t e^{\alpha u}B_u^H du + vB_t^H)(-\alpha ve^{-\alpha s} \int_0^s e^{\alpha v}B_v^H dv + vB_s^H)] \\ &= -\frac{\alpha v^2}{2}e^{-\alpha t} \int_0^t e^{\alpha u}(u^{2H} + s^{2H} - |u - s|^{2H})du \\ &\quad - \frac{\alpha v^2}{2}e^{-\alpha s} \int_0^s e^{\alpha v}(v^{2H} + t^{2H} - |v - t|^{2H})dv + \frac{v^2}{2}(t^{2H} + s^{2H} - |t - s|^{2H}) \\ &\quad + \frac{\alpha^2 v^2}{2}e^{-\alpha t - \alpha s} \int_0^t \int_0^s e^{\alpha u + \alpha v}(u^{2H} + v^{2H} - |u - v|^{2H})dudv = \frac{v^2}{2} \sum_{n=1}^{10} I_n \end{aligned} \tag{A2}$$

with

$$\begin{aligned} I_1 &= -\alpha e^{-\alpha t} \int_0^t e^{\alpha u}s^{2H}du, I_2 = -\alpha e^{-\alpha t} \int_0^t e^{\alpha u}u^{2H}du, I_3 = \alpha e^{-\alpha t} \int_0^t e^{\alpha u}|u - s|^{2H}du \\ I_4 &= -\alpha e^{-\alpha s} \int_0^s e^{\alpha v}t^{2H}dv, I_5 = -\alpha e^{-\alpha s} \int_0^s e^{\alpha v}v^{2H}dv, I_6 = \alpha e^{-\alpha s} \int_0^s e^{\alpha v}(t - v)^{2H}dv \\ I_7 &= t^{2H} + s^{2H} - (t - s)^{2H}, I_8 = \alpha^2 e^{-\alpha t - \alpha s} \int_0^t e^{\alpha v}dv \int_0^s e^{\alpha u}u^{2H}du \\ I_9 &= \alpha^2 e^{-\alpha t - \alpha s} \int_0^t e^{\alpha u}du \int_0^s e^{\alpha v}v^{2H}dv \\ I_{10} &= -\alpha^2 e^{-\alpha t - \alpha s} \int_0^t \int_0^s e^{\alpha u + \alpha v}|u - v|^{2H}dudv \end{aligned}$$

The first two integrals are equal to:

$$I_1 = s^{2H}(e^{-\alpha t} - 1) \text{ and } I_2 = -e^{-\alpha t} \int_0^t u^{2H}de^{\alpha u} = -t^{2H} + 2He^{-\alpha t} \int_0^t e^{\alpha u}u^{2H-1}du$$

By changing variables and integration by parts, we can obtain:

$$\begin{aligned} I_3 &= \alpha e^{-\alpha t} \int_0^s e^{\alpha u}(s - u)^{2H}du + \alpha e^{-\alpha t} \int_s^t e^{\alpha u}(u - s)^{2H}du \\ &= \alpha e^{-\alpha t + \alpha s} \int_0^s e^{-\alpha z}z^{2H}dz + \alpha e^{-\alpha t + \alpha s} \int_0^{t-s} e^{\alpha z}z^{2H}dz \\ &= -e^{-\alpha t + \alpha s} \left(e^{-\alpha s}s^{2H} - 2H \int_0^s e^{-\alpha z}z^{2H-1}dz - e^{\alpha(t-s)}(t - s)^{2H} \right. \\ &\quad \left. + 2H \int_0^{t-s} e^{\alpha z}z^{2H-1}dz \right) \\ &= -e^{-\alpha t}s^{2H} + (t - s)^{2H} + 2He^{-\alpha t + \alpha s} \int_0^s e^{-\alpha z}z^{2H-1}dz \\ &\quad - 2He^{-\alpha t + \alpha s} \int_0^{t-s} e^{\alpha z}z^{2H-1}dz. \end{aligned}$$

Similarly, we can have:

$$\begin{aligned}
 I_4 &= t^{2H}(e^{-\alpha s} - 1), I_5 = -s^{2H} + 2He^{-\alpha s} \int_0^s e^{\alpha v} v^{2H-1} dv \\
 I_6 &= \alpha e^{-\alpha s + \alpha t} \int_{t-s}^t e^{-\alpha z} z^{2H} dz = -e^{-\alpha s + \alpha t} \int_{t-s}^t z^{2H} de^{-\alpha z} \\
 &= -e^{-\alpha s} t^{2H} + (t-s)^{2H} + 2He^{-\alpha s + \alpha t} \int_{t-s}^t e^{-\alpha z} z^{2H-1} dz \\
 I_8 &= e^{-\alpha t - \alpha s} (e^{\alpha t} - 1) \int_0^s u^{2H} de^{\alpha u} = (1 - e^{-\alpha t}) s^{2H} - 2He^{-\alpha s} (1 - e^{-\alpha t}) \int_0^s e^{\alpha u} u^{2H-1} du \\
 I_9 &= (1 - e^{-\alpha s}) t^{2H} - 2He^{-\alpha t} (1 - e^{-\alpha s}) \int_0^t e^{\alpha v} v^{2H-1} dv
 \end{aligned}$$

Then, we consider the term I_{10} , which can be represented as:

$$\begin{aligned}
 I_{10} &= -\alpha^2 e^{-\alpha t - \alpha s} \int_0^s \int_0^v e^{\alpha u + \alpha v} (v - u)^{2H} dudv \\
 &\quad -\alpha^2 e^{-\alpha t - \alpha s} \int_0^s \int_v^s e^{\alpha u + \alpha v} (u - v)^{2H} dudv \\
 &\quad -\alpha^2 e^{-\alpha t - \alpha s} \int_s^t \int_0^s e^{\alpha u + \alpha v} (v - u)^{2H} dudv \\
 &= -2\alpha^2 e^{-\alpha t - \alpha s} \int_0^s \int_0^v e^{\alpha u + \alpha v} (v - u)^{2H} dudv \\
 &\quad -\alpha^2 e^{-\alpha t - \alpha s} \int_s^t \int_0^s e^{\alpha u + \alpha v} (v - u)^{2H} dudv \\
 &= I_{10}^1 + I_{10}^2
 \end{aligned}$$

Using the change of variables $u - v = z$, the change of order of integration, and integration by parts, we obtain:

$$\begin{aligned}
 I_{10}^1 &= -2\alpha^2 e^{-\alpha t - \alpha s} \int_0^s e^{2\alpha v} \int_0^v e^{-\alpha z} z^{2H} dz dv \\
 &= -2\alpha^2 e^{-\alpha t - \alpha s} \int_0^s e^{-\alpha z} z^{2H} \int_z^s e^{2\alpha v} dv dz \\
 &= -2\alpha^2 e^{-\alpha t - \alpha s} \int_0^s e^{-\alpha z} z^{2H} \frac{e^{2\alpha s} - e^{2\alpha z}}{2\alpha} dz \\
 &= -\alpha e^{-\alpha t + \alpha s} \left(\int_0^s e^{-\alpha z} z^{2H} dz - \int_0^s e^{\alpha u} u^{2H} du \right) \\
 &= e^{-\alpha t} s^{2H} - 2He^{-\alpha t + \alpha s} \int_0^s e^{-\alpha z} z^{2H-1} dz + e^{-\alpha t} s^{2H} - 2He^{-\alpha t - \alpha s} \int_0^s e^{\alpha u} u^{2H-1} du
 \end{aligned}$$

Now, we consider I_{10}^2 , First we deal with the case of $t > 2s$. Using the change of variables $u - v = z$ in the inner integral, changing the order of integration, and integrating with respect to v , we obtain:

$$\begin{aligned}
 I_{10}^2 &= -\alpha^2 e^{-\alpha t - \alpha s} \int_s^t \int_{v-s}^v e^{-\alpha z + 2\alpha v} z^{2H} dz dv \\
 &= -\alpha^2 e^{-\alpha t - \alpha s} \left(\int_0^s \int_s^{z+s} e^{-\alpha z + 2\alpha v} z^{2H} dv dz + \int_s^{t-s} \int_z^{z+s} e^{-\alpha z + 2\alpha v} z^{2H} dv dz \right. \\
 &\quad \left. + \int_{t-s}^t \int_z^t e^{-\alpha z + 2\alpha v} z^{2H} dv dz \right) \\
 &= -\alpha^2 e^{-\alpha t - \alpha s} \left(\int_0^s e^{-\alpha z} z^{2H} \frac{e^{2\alpha(z+s)} - e^{2\alpha s}}{2\alpha} dz \right. \\
 &\quad \left. + \int_s^{t-s} e^{-\alpha z} z^{2H} \frac{e^{2\alpha(z+s)} - e^{2\alpha z}}{2\alpha} dz + \int_{t-s}^t e^{-\alpha z} z^{2H} \frac{e^{2\alpha t} - e^{2\alpha z}}{2\alpha} dz \right) \\
 &= \frac{-\alpha}{2} e^{-\alpha t + \alpha s} \int_0^{t-s} e^{\alpha z} z^{2H} dz - \frac{\alpha}{2} e^{-\alpha t - \alpha s} \int_s^t e^{\alpha z} z^{2H} dz - \frac{\alpha}{2} e^{-\alpha t + \alpha s} \int_0^s e^{-\alpha z} z^{2H} dz \\
 &\quad + \frac{-\alpha}{2} e^{-\alpha s + \alpha t} \int_{t-s}^t e^{-\alpha z} z^{2H} dz \\
 &= e^{-\alpha s} t^{2H} - e^{-\alpha t} s^{2H} - He^{-\alpha s + \alpha t} \int_{t-s}^t e^{-\alpha z} z^{2H-1} dz + He^{-\alpha t + \alpha s} \int_0^s e^{-\alpha z} z^{2H-1} dz \\
 &\quad - He^{-\alpha t - \alpha s} \int_s^t e^{\alpha z} z^{2H-1} dz + He^{-\alpha t + \alpha s} \int_0^{t-s} e^{\alpha z} z^{2H-1} dz - (t-s)^{2H}
 \end{aligned}$$

Similarly, one can verify that the above formula follows in the case of $s < t < 2s$. Finally, summing up all the terms, we obtain:

$$\begin{aligned} \text{Cov}(X_t, X_s) &= \text{Cov}(\tilde{X}_t, \tilde{X}_s) \\ &= \frac{Hv^2}{2} (-e^{-\alpha t+\alpha s} \int_0^{t-s} e^{\alpha z} z^{2H-1} dz + e^{\alpha t-\alpha s} \int_{t-s}^t e^{-\alpha z} z^{2H-1} dz \\ &\quad - e^{-\alpha t-\alpha s} \int_s^t e^{\alpha z} z^{2H-1} dz + e^{-\alpha t+\alpha s} \int_0^s e^{-\alpha z} z^{2H-1} dz \\ &\quad + 2e^{-\alpha t-\alpha s} \int_0^t e^{\alpha z} z^{2H-1} dz) \end{aligned} \tag{A3}$$

Moreover, using (A3), for all $H \in (0, 1)$, we have:

$$\text{Var}X_t = \text{Var}\tilde{X}_t = Hv^2 \int_0^t z^{2H-1} (e^{-\alpha z} + e^{-\alpha(2t-z)}) dz \tag{A4}$$

Which implies (4). □

Proof of Lemma 2. From (A1), we can easily obtain:

$$\mathbb{E}[X_t] = m(1 - e^{-\alpha t}) + X_0 e^{-\alpha t} \tag{A5}$$

Moreover, using (4) in Lemma 1, we have:

$$\text{Var}[X_t] = Hv^2 \int_0^t z^{2H-1} (e^{-\alpha z} + e^{-\alpha(2t-z)}) dz \rightarrow \frac{H\Gamma(2H)}{\alpha^{2H}} \tag{A6}$$

where $\alpha > 0$ as $t \rightarrow \infty$.

Since the random variable X_t has normal distribution, we can obtain (5) using (A5) and (A6). Now, we consider (6). For convenience, we assume $t \geq s \geq 0$ and $p = 2$. Thus, we show that

$$\mathbb{E}(X_t - X_s)^2 \leq C|t - s|^{2H} \tag{A7}$$

Using the fact $X_t = X_0 + \alpha \int_0^t (m - X_s) ds + vB_t^H$, we obtain:

$$|X_t - X_s| \leq |\alpha m(t - s)| + \alpha \int_s^t |X_u| du + v|B_t^H - B_s^H| \tag{A8}$$

Therefore, using (5), we obtain:

$$\begin{aligned} \mathbb{E}(X_t - X_s)^2 &\leq 3|\alpha m(t - s)|^2 + 3|\alpha|^2 \mathbb{E}(\int_s^t |X_u| du)^2 + 3v^2 \mathbb{E}(B_t^H - B_s^H)^2 \\ &\leq 3|\alpha m(t - s)|^2 + 3|\alpha|^2 (t - s) \int_s^t \mathbb{E}|X_u|^2 du + 3v^2 (t - s)^{2H} \\ &\leq C|t - s|^2 \end{aligned}$$

Thus, (A7) is proved. Since $X_t - X_s$ has a normal distribution, (6) follows from (A7) in the standard way. □

Proof of Lemma 3. First, using (5) and (A6), one can easily check the condition

$$\mathbb{E}[\sigma_t^2] = \mathbb{E}[e^{2X_t}] = e^{2\mathbb{E}[X_t] + 2\text{Var}[X_t]} \leq C$$

Which implies:

$$\sup_{0 \leq t \leq T} |\sigma_t^2| = O_p(1) \tag{A9}$$

From (A9), we can see that the second condition of A1 in Hypothesis 1 is satisfied. Since e^y is a continuous function of y and X_t is $H - \epsilon$ Hölder continuous with any small ϵ , using Lemma 2 and (A9), we have:

$$E|\sigma_t - \sigma_s| = E|e^{X_t} - e^{X_s}| = E|e^{X_s} (e^{X_t - X_s} - 1)| \leq e^{X_s} (e^{C|t-s|^{pH}} - 1) \leq C|t - s|^{pH} \tag{A10}$$

Which implies $\sup\{|\sigma_s - \sigma_t|, |s - t| \leq a\} = O_{\mathbb{P}}(a^{1/2} |\log(a)|^{1/2})$. Hence the condition of A1 in Hypothesis 1 is satisfied. For the condition A2 in Hypothesis 1, using (A10), we obtain:

$$\sup\left|\int_{t_{i-1}}^{t_i} (\sigma(s) - \sigma(t_{i-1}))dW_s\right|^2 \leq 2\log(n)\sup\left|\int_{t_{i-1}}^{t_i} (\sigma(s) - \sigma(t_{i-1}))^2 ds\right| \leq \frac{C \log(n)}{n^2}$$

Which implies A2 in Hypothesis 1. \square

Proof of Proposition 1. From Lemma 3, we can see that assumptions A1 and A2 of σ_t in Hypothesis 1 are satisfied for the volatility process in (1). From the definition of M_n , we can see that M_n has the same asymptotic distribution as $\sup_{0 \leq t \leq T} |\sigma_t^2|$. Hence, we can obtain

the desired results. \square

References

- Black, F.; Scholes, M. The Pricing of Options and Corporate Liabilities. *J. Political Econ.* **1973**, *81*, 637–654. [\[CrossRef\]](#)
- Fouque, J.-P.; Papanicolaou, G.; Sircar, K.R. *Derivatives in Financial Markets with Stochastic Volatility*; Cambridge University Press: Cambridge, UK, 2000.
- Hull, J.; White, A. The pricing of options on assets with stochastic volatilities. *J. Financ.* **1987**, *42*, 281–300. [\[CrossRef\]](#)
- Scott, L.O. Option Pricing when the Variance Changes Randomly: Theory, Estimation, and an Application. *J. Financ. Quant. Anal.* **1987**, *22*, 419. [\[CrossRef\]](#)
- Stein, E.M.; Stein, J.C. Stock Price Distributions with Stochastic Volatility: An Analytic Approach. *Rev. Financ. Stud.* **1991**, *4*, 727–752. [\[CrossRef\]](#)
- Comte, F.; Renault, E. Long memory in continuous-time stochastic volatility models. *Math. Financ.* **1998**, *8*, 291–323. [\[CrossRef\]](#)
- Comte, F.; Coutin, L.; Renault, E. Affine fractional stochastic volatility models. *Ann. Financ.* **2012**, *8*, 337–378. [\[CrossRef\]](#)
- Chronopoulou, A.; Viens, F.G. Estimation and pricing under long-memory stochastic volatility. *Ann. Financ.* **2012**, *8*, 379–403. [\[CrossRef\]](#)
- Chronopoulou, A.; Viens, F.G. Stochastic volatility and option pricing with long-memory in discrete and continuous time. *Quant. Financ.* **2012**, *12*, 635–649. [\[CrossRef\]](#)
- Xiao, W.; Yu, J. Asymptotic theory for estimating drift parameters in the fractional vasicek model. *Econ. Theory* **2019**, *35*, 198–231. [\[CrossRef\]](#)
- Bennedsen, M.; Lunde, A.; Pakkanen, M.S. Decoupling the Short- and Long-Term Behavior of Stochastic Volatility. *J. Financ. Econ.* **2021**, 1–46. [\[CrossRef\]](#)
- Bayer, C.; Friz, P.; Gatheral, J. Pricing under rough volatility. *Quant. Financ.* **2016**, *16*, 887–904. [\[CrossRef\]](#)
- Gatheral, J.; Jaisson, T.; Rosenbaum, M. Volatility is rough. *Quant. Financ.* **2018**, *18*, 933–949. [\[CrossRef\]](#)
- Livieri, G.; Mouti, S.; Pallavicini, A.; Rosenbaum, M. Rough volatility: Evidence from option prices. *IJSE Trans.* **2018**, *50*, 767–776. [\[CrossRef\]](#)
- El Euch, O.; Rosenbaum, M. The characteristic function of rough Heston models. *Math. Financ.* **2019**, *29*, 3–38. [\[CrossRef\]](#)
- Alòs, E.; León, J.A.; Vives, J. On the short-time behavior of the implied volatility for jump-diffusion models with stochastic volatility. *Financ. Stoch.* **2007**, *11*, 571–589. [\[CrossRef\]](#)
- Fukasawa, M.; Takabatake, T. Asymptotically efficient estimators for self-similar stationary Gaussian noises under high frequency observations. *Bernoulli* **2019**, *25*, 1870–1900. [\[CrossRef\]](#)
- Li, X.; Wei, Y.; Chen, X.; Ma, F.; Liang, C.; Chen, W. Which uncertainty is powerful to forecast crude oil market volatility? New evidence. *Int. J. Financ. Econ.* **2020**, 1–19. [\[CrossRef\]](#)
- Wang, D.; Xin, Y.; Chang, X.; Su, X. Realized volatility forecasting and volatility spillovers: Evidence from Chinese non-ferrous metals futures. *Int. J. Financ. Econ.* **2020**, *26*, 2713–2731. [\[CrossRef\]](#)
- Wang, X.; Xiao, W.; Yu, J. Modeling and forecasting realized volatility with the fractional Ornstein–Uhlenbeck process. *J. Econ.* **2021**. [\[CrossRef\]](#)
- Da Fonseca, J.; Zhang, W. Volatility of volatility is (also) rough. *J. Futur. Mark.* **2019**, *39*, 600–611. [\[CrossRef\]](#)
- Cao, J.; Kim, J.-H.; Kim, S.-W.; Zhang, W. Rough stochastic elasticity of variance and option pricing. *Financ. Res. Lett.* **2019**, *37*, 101381. [\[CrossRef\]](#)
- Takaishi, T. Rough volatility of Bitcoin. *Financ. Res. Lett.* **2019**, *32*, 101379. [\[CrossRef\]](#)
- Fukasawa, M.; Takabatake, T.; Westphal, R. Is volatility rough? *arXiv* **2019**, arXiv:1905.04852.
- Brandi, G.; Di Matteo, T. Multiscaling and rough volatility: An empirical investigation. *arXiv* **2022**, arXiv:2201.10466.
- Alòs, E.; León, J. An Intuitive Introduction to Fractional and Rough Volatilities. *Mathematics* **2021**, *9*, 994. [\[CrossRef\]](#)
- Jacod, J.; Todorov, V. Testing for common arrivals of jumps for discretely observed multidimensional processes. *Ann. Stat.* **2009**, *37*, 1792–1838. [\[CrossRef\]](#)

28. Fan, J.; Wang, Y. Spot volatility estimation for high-frequency data. *Stat. Interface* **2008**, *1*, 279–288. [[CrossRef](#)]
29. Renò, R. Nonparametric estimation of the diffusion coefficient of stochastic volatility models. *Econ. Theory* **2008**, *24*, 1174–1206. [[CrossRef](#)]
30. Kantelhardt, J.W.; Zschiegner, S.A.; Koscielny-Bunde, E.; Havlin, S.; Bunde, A.; Stanley, H. Multifractal detrended fluctuation analysis of nonstationary time series. *Phys. A Stat. Mech. Appl.* **2002**, *316*, 87–114. [[CrossRef](#)]
31. Berzin, C.; Latour, A.; León, J.R. *Inference on the Hurst Parameter and the Variance of Diffusions Driven by Fractional Brownian Motion*; Springer: Cham, Switzerland, 2014; Volume 216, p. 200.
32. Guennoun, H.; Jacquier, A.; Roome, P.; Shi, F. Asymptotic Behavior of the Fractional Heston Model. *SIAM J. Financ. Math.* **2018**, *9*, 1017–1045. [[CrossRef](#)]
33. Funahashi, H.; Kijima, M. Does the Hurst index matter for option prices under fractional volatility? *Ann. Financ.* **2017**, *13*, 55–74. [[CrossRef](#)]
34. Neuenkirch, A.; Shalaiko, T. The order barrier for strong approximation of rough volatility models. *arXiv* **2016**, arXiv:1606.03854.
35. Kermarrec, G. On Estimating the Hurst Parameter from Least-Squares Residuals. Case Study: Correlated Terrestrial Laser Scanner Range Noise. *Mathematics* **2020**, *8*, 674. [[CrossRef](#)]
36. Jena, S.K.; Tiwari, A.K.; Dogan, B.; Hammoudeh, S. Are the top six cryptocurrencies efficient? evidence from time-varying long memory. *Int. J. Financ. Econ.* **2020**. [[CrossRef](#)]
37. Xiao, W.; Zhang, W.; Xu, W. Parameter estimation for fractional Ornstein–Uhlenbeck processes at discrete observation. *Appl. Math. Model.* **2011**, *35*, 4196–4207. [[CrossRef](#)]
38. Christensen, K.; Oomen, R.C.; Podolskij, M. Fact or friction: Jumps at ultra high frequency. *J. Financ. Econ.* **2014**, *114*, 576–599. [[CrossRef](#)]
39. Cheridito, P.; Kawaguchi, H.; Maejima, M. Fractional Ornstein-Uhlenbeck processes. *Electron. J. Probab.* **2003**, *8*, 1–14. [[CrossRef](#)]
40. Kubilius, K. CLT for quadratic variation of Gaussian processes and its application to the estimation of the Orey index. *Stat. Probab. Lett.* **2020**, *165*, 108845. [[CrossRef](#)]